Natural Resources Canada | Ressources naturelles Canada

GEOLOGICAL SURVEY OF CANADA
OPEN FILE 7768

Downhole geophysical data collected in 11 boreholes near St-Édouard-de-Lotbinière, Quebec

H.L. Crow, P. Ladevèze

2015

Canada

GEOLOGICAL SURVEY OF CANADA
OPEN FILE 7768

Downhole geophysical data collected in 11 boreholes near St-Édouard-de-Lotbinière, Quebec

H.L. Crow[1], P. Ladevèze[2]

[1] Geological Survey of Canada, Ottawa, Ontario

[2] Institut national de la recherche scientifique (INRS), Québec, Quebec

2015

doi:10.4095/297047

This publication is available for free download through GEOSCAN (http://geoscan.nrcan.gc.ca/).

Recommended citation
Crow, H.L. and Ladevèze, P., 2015. Downhole geophysical data collected in 11 boreholes near St-Édouard-de-Lotbinière, Quebec; Geological Survey of Canada, Open File 7768, 1 .zip file. doi:10.4095/297047

Publications in this series have not been edited; they are released as submitted by the author.

Contents

1.0 Introduction

The Geological Survey of Canada (GSC) is investigating potential links between a deep gas-bearing shale formation and shallow aquifers in the St. Lawrence Lowlands, southern Québec. The study site is located near two industry gas wells (A268 and A275) drilled in the Utica Shale and fracked in 2009-2010. This project integrates hydrogeological, geophysical, geochemical, and geomechanical datasets to obtain indirect data on the cap rock - the protective unit located between the shallow bedrock aquifers and the gas-bearing Utica Shale located 1500 to 2000 m below the surface. Information on cap rock integrity could support the development of provincial regulations and water management plans to ensure that aquifers will not be adversely affected by shale gas development (Lavoie et al., 2014).

To support the project's near-surface hydrogeological, geochemical, and structural studies, downhole geophysical logs were collected in 11 GSC-drilled boreholes in the St-Édouard region, located ~65 km east of Quebec City. Well depths ranged from 30 to 148 m. The suite of logs included:

- natural gamma and guard resistivity logs to identify lithological variations;
- optical and acoustic televiewer images to analyze the orientations of structural features and identify fractures;
- fluid temperature/conductivity logs and pumped heat pulse flow meter (HPFM) testing to identify fractures transmitting fluid, and
- full waveform sonic logs to compute compressional (P-) and shear (S-) wave velocities in the bedrock.

This report summarises the logging procedures and data analyses carried out, and presents the factual results of the logging conducted in 2013 and 2014. Additional details on the logging techniques used during this project are provided in Appendix A. Figures presenting the suite of geophysical logs collected in each borehole are found in Appendix B, and the digital dataset can be found in Appendix C. This dataset consists of .LAS files of the log suites, excel spreadsheets of flow meter test results, and WellCAD files of televiewer images. WellCAD files can be viewed by downloading the free WellCAD Reader software at http://www.alt.lu/downloads.htm.

Results of these downhole surveys are being integrated into several aspects of the project. Fluid logs and HPFM test results were used on-site to provide water sampling depths where the boreholes intersected flowing fractures. Sonic velocities were compared with industry acoustic logs collected in deep boreholes to understand how geomechanical properties vary between shallow (0 - 150 m) and deep (150 - 700 m) geological formations (Séjourné, 2015). Finally, results of the televiewer structural analyses will be compared to measurements of structural orientations from local outcrops, and to structures interpreted from formation microimager (FMI) logs from deep industry wells to investigate the continuity of structural features.

1.1 Recent Local Borehole Geophysical Studies

Within the framework of a hydrogeological characterization study in the Montérégie Est region in southern Quebec, a borehole geophysical study was carried out in 2011 in twelve shallow bedrock boreholes (23 m - 146 m). This project was carried out in partnership with the Institut national de la recherche scientifique - Centre Eau Terre Environnement (INRS-ETE). The objective of the logging was to provide the groundwater study with a high-quality dataset of downhole geophysical and

hydrogeological information using a suite of tools which included the magnetic susceptibility, natural gamma, apparent conductivity, fluid temperature, heat pulse flow meter, and acoustic televiewer (Crow et al., 2012). Although very few of the fractures were found to be transmitting groundwater, flowing fractures were primarily bedding-parallel. Four main fracture sets were present with a common NNE to NE average strike direction that agrees with the regional strike of the St. Lawrence Platform and Appalachians main structures. The dataset was integrated into a 2D numerical model of the fractured-rock aquifer system which aimed to provide an understanding of present day groundwater flow dynamics, and of the evolution of flow through recent geologic time (Laurencelle et al., 2013).

In recent years, concerns voiced in Quebec over potential groundwater contamination related to petroleum exploration and unconventional hydrocarbon extraction led INRS-ETE to conduct an investigation of a potential link between an 800 m deep petroleum reservoir and a shallow fractured rock aquifer system in the Haldimand Sector of Gaspé, Québec. To support the study, the GSC collected geophysical logs in 10 open rock and 3 PVC-cased wells, ranging in depth from 36 m – 52m, during the fall of 2012. Logs were acquired to better understand the lithological variations in the near-surface sedimentary rock, *in situ* variation in fluid temperature & conductivity, flow rates and direction of flow along the wellbore, and the structural orientations of fractures intersected by the boreholes (Crow et al., 2013). These results indicated that bedrock fractures are most frequent in the upper 15 m of the rock aquifer and that this zone controls the groundwater flow in the region. These conditions, along with hydrochemical results from ground and surface water samples were used to develop a 2D vertical model of shallow and deep groundwater flow patterns (Raynaud et al., 2013; MDDELCC, 2014). The results of this integrated study are helping to assess potential risks to groundwater quality caused by local industry activities. Similar techniques are being applied to the present study in St-Édouard.

1.2 Geological context

The St-Édouard area is located at the junction of three tectonostratigraphic domains: the autochthonous and parautochthonous domains of the St. Lawrence Platform, and the allochthonous domain of the external Humber Zone (from northwest to southeast) (St.-Julien and Hubert, 1975; Williams, 1979; Castonguay et al., 2010). The domains and locations of the logged boreholes are presented in Figure 1.

The autochthonous domain includes rocks of the St. Lawrence sedimentary platform deposited in a foreland basin setting (Lavoie, 2008). Rocks are slightly deformed in the Chambly-Fortierville syncline. This fold is striking northeast and is asymmetric: in the southern flank, the beds dip more steeply than in the northern flank. Units in the St-Édouard area are siliciclastic rocks such as interbedded grey-black shale, sandstone, and siltstone (Nicolet & Pontgavré Formations; Lorraine Group; Upper Ordovician) (Clark and Globensky, 1973; Globensky, 1987). To the north of the Jacques-Cartier normal fault, shales with thin interbeds of calcareous siltstones are outcropping (Lotbinière Formation; Ste.-Rosalie Group; Middle – Upper Ordovician) (Belt et al., 1979; Clark and Globensky, 1973).

The parautochthonous domain is located between two regional thrusts faults: the Aston fault and Logan's Line. This is where Talisman well A275 is located. This domain is a southeast-dipping system of thrust faults that display imbricated thrust fan geometries made up of platform (autochthonous) rocks (Castonguay et al., 2006; Séjourné et al., 2003; St.-Julien et al., 1983). Within this area, rocks are also affected by large-scale northeast-striking slightly overturned folds (Comeau et

al., 2004). Lithologies are mainly composed of mudstone and fine- to coarse-grained sandstones with less abundant fine-grained limestones and conglomerate (Les Fonds Formation - a time-stratigraphic equivalent of the Utica Shales - Ste.-Rosalie Group; Upper Ordovician) (Comeau et al., 2004).

The allochthonous zone is composed of exotic (non-autochthonous) formations northwestwardly-displaced along the Appalachians thrusts sheets. The Cambrian-Ordovician allochthonous rocks structurally overlie the parautochthonous domain east of Logan's Line (Séjourné et al., 2003). Units outcroping in the area are mostly black shales with interbeds of argillaceous limestone, dolomite and sandstone, and local beds of limestone (Bourret Formation; Laurier Group; Middle Ordovician) (Clark and Globensky, 1973; Clark and Globensky, 1976).

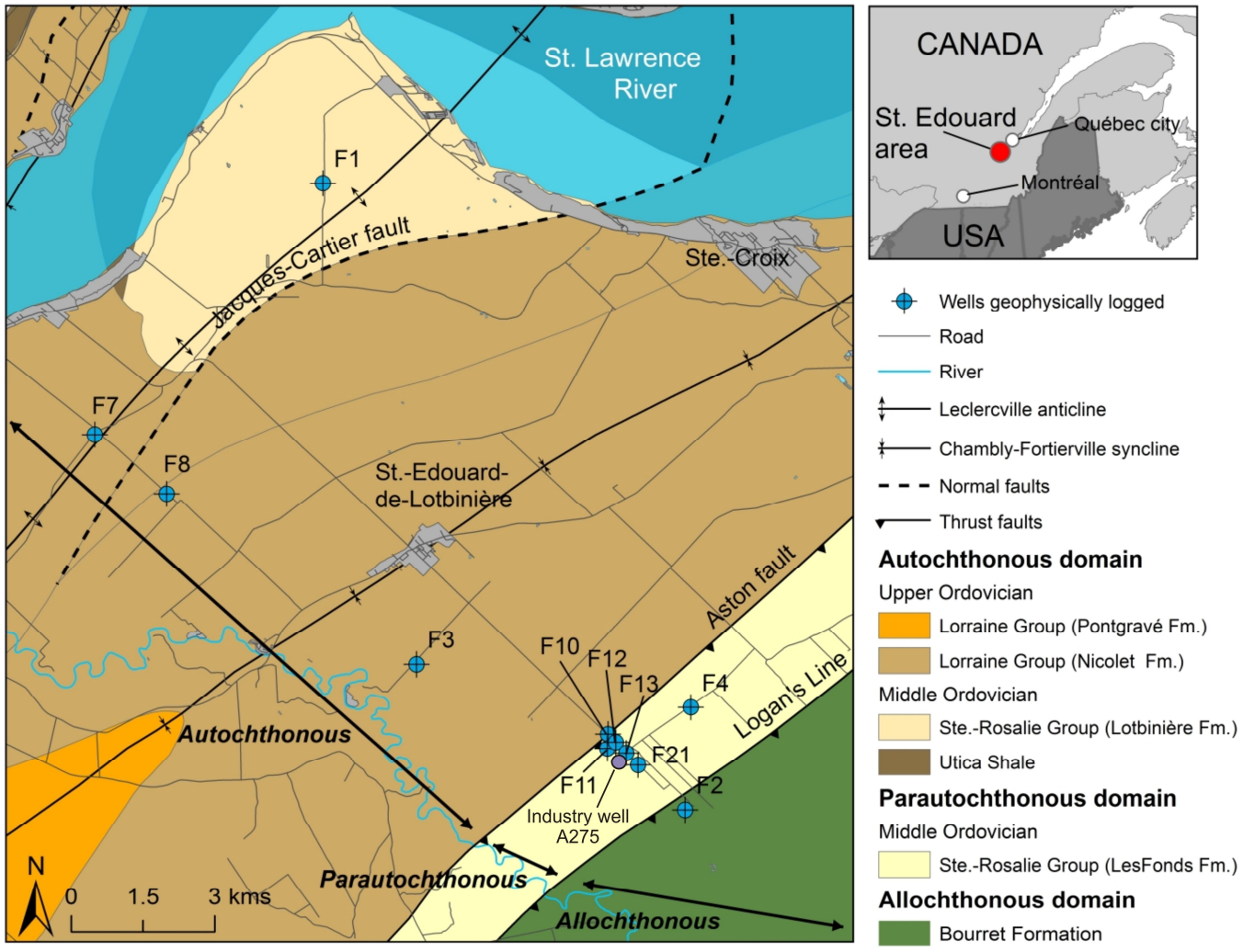

Figure 1 - Location of the study area, ~65 km east of Quebec City, showing the local towns and the geological formations in the study area (Geological map of Québec from Thériault and Beauséjour (2012)).

2.0 Fieldwork

2.1 Drilling Methods and sample collection

Drilling operations were supervised by GSC personnel in the fall of 2013 and 2014. Boreholes F-1, -2, -3, -4, -7, -8 and -21 were diamond drilled by Forages Comeau Inc. using a geotechnical drill rig. Bedrock cores were collected along the entire borehole lengths. The remaining wells (F-10, -11, -12, and -13) were rotary drilled in 2014 by Forages LBM Inc. using a Foremost DR-12W drill rig. Cuttings were collected during the drilling for lithological identification. A summary table of the borehole details can be found in Table 1. Co-ordinates of the borehole locations can be found on the log figures in Appendix B.

Upon completion of drilling, boreholes were not flushed with fresh water to avoid removing gases or diluting native connate pore fluids which escaped during the drilling. The use of a high-pressure air pump was preferred to lift the fluids out of the borehole. This was done to allow for clearer borehole fluids to replace cloudy drilling fluids for the optical image logging.

Table 1. Basic borehole information for the logged wells. bgl=below ground level.

Borehole ID	Municipality (QC)	Drilling Method	Diameter (mm)	Drilling Year	Depth to Bedrock (m bgl)	Depth geophys. logged (Max depth drilled) (m bgl)
F-1	Lotbinière	Diamond drill, Cored	96	2013	2.59	48.97 (49.7)
F-2	St-Édouard	Diamond drill, Cored	96	2013	6.1	48.49 (52.12)
F-3	St-Édouard	Diamond drill, Cored	96	2013	20.12	49.69 (49.9)
F-4	St-Édouard	Diamond drill, Cored	96	2013	39.60	60.00 (60.4)
F-7	Lotbinière	Diamond drill, Cored	96	2014	11.43	49.99 (51.51)
F-8	Lotbinière	Diamond drill, Cored	96	2014	1.43	50.68 (51.51)
F-10	St-Édouard	Rotary	152	2014	15.85	29.00 (30.48)
F-11	St-Édouard	Rotary	152	2014	6.4	45.97 (54.86)
F-12	St-Édouard	Rotary	152	2014	7.92	70.50 (73.15)
F-13	St-Édouard	Rotary	152	2014	1.83	50.67 (60.96)
F-21	St-Édouard	Diamond drill, Cored	96	2014	3.66	147.95 (152.1)

2.2 Geophysical Logging

The first phase of the fieldwork (logging of boreholes F-1, -2, -3, and -4) was completed between October 20th and 26th, 2013. The second phase of fieldwork (remaining boreholes and some relogging of 2013 boreholes) was carried out between October 31st and November 11th, 2014. The suite of tools used in all the boreholes consisted of natural gamma, guard resistivity, optical and acoustic televiewers, full waveform sonic, fluid temperature and fluid conductivity, and heat-pulse flowmeter. Table 2 contains a summary of the logs collected in each borehole, and Table 3 describes each tool's logging unit, data resolution, logging details, and the practical interpretation of each log. More detailed information on each tool can be found in Appendix A.

Geophysical logs provide a means of identifying and characterizing lithological units based on variations in their chemical and physical properties. The logs collectively termed "**lithological logs**" (natural gamma and guard resistivity) augment geological interpretation, and permit fine tuning of geological contact depths when core or cuttings are collected. Lithological interpretation was also supported by the sonic and televiewer logs.

The group of logs known as "**structural** or **geomechanical**" includes acoustic (ATV) and optical (OTV) televiewers, and full waveform sonic (FWS) logs. The televiewers record high-resolution 360º unwrapped images of the inside of the borehole wall. The ATV records the amplitude and traveltime of reflected ultrasonic beams emitted from a high-frequency transmitter. This allows for an analysis of the wall roughness, orientation of structural features (strike direction, dip), borehole diameter, and estimation of the fracture aperture at the borehole wall. The optical televiewer (OTV) collects a digital color image of the inside of the borehole wall. In clear borehole fluid, the tool can be calibrated to render a true color image, although in cloudy fluid, the image becomes increasingly obscured.

The FWS tool uses a 15 kHz transmitter at the base of a centralized sonic probe to emit pulses of mechanical energy into a fluid filled borehole. The compressional energy is refracted at the borehole wall as compressional (P) and shear (S) head waves, and reflected as numerous modes which are recorded by three receivers on the probe. In full waveform sonic logging, the full wavetrain is recorded, allowing for a calculation of shear (S) wave velocity through later arrivals in the signal, in addition to a measure of compressional (P) wave velocities through interpretation of the first arrivals.

Finally, the suite of logs known together as "**hydrogeophysical**" (fluid temperature & conductivity, flowmeter) detect fluid movement within the open wellbore, allowing for the inference of groundwater movement and flowing fractures. The televiewer logs and caliper can also be considered hydrogeophysical in groundwater studies.

Table 2. Geophysical logs collected in St-Édouard and region.

BH	Geophysical logs						
	Lithological		Structural/Geomechanical			Hydrogeophysical	
	Natural gamma	Resistivity	Optical Televiewer	Acoustic Televiewer & caliper	Full waveform sonic	Fluid temp. & cond.	Heat pulse flow meter
F-1	✓	✓	✓	✓	✓	✓	✓
F-2	✓	✓	Fluid cloudy	✓	✓	✓	✓
F-3	✓	✓	✓	✓	✓	✓	✓
F-4	✓	✓	✓	✓	✓	✓	✓
F-7	✓	✓	✓	✓	✓	✓	✓
F-8	✓	✓	✓	✓	✓	✓	✓
F-10	✓	✓	Fluid cloudy	✓	✓	✓	Not conducted in rotary holes
F-11	✓	✓		✓	✓	✓	
F-12	✓	✓		✓	✓	✓	
F-13	✓	✓		✓	✓	✓	
F-21	✓	✓	✓	✓	✓	✓	✓

Table 3. Summary of the downhole log suite, including logging unit, data resolution, logging details, and practical interpretations of each log. Table abbreviations: Req=requires, Cent=centralization

Downhole Geophysical Log *[Manufacturer]*	**Req. Fluid**	**Req. Cent.**	**Logging Unit**	**Radius of Investigation** ***[Vertical resolution]***	**Logging Speed**	**Logging Interval**	**Practical interpretations in open rock**
Spectral Gamma *[Mount Sopris]*			Counts per second (cps)	0.3 - 0.6 m *[centimetres, function of logging speed]*	1 m/min	0.01 m	Relative grain-size, lithological boundaries
Guard Resistivity *[Mount Sopris]*	✓	Req. decentralization	Ohm-metres (Ohm-m)	0.15 – 0.20 m *[2 cm]*	3 m/min	0.02 m	Relative formation resistivity, lithological boundaries
Optical Televiewer *[Advanced Logic Technology/ Mount Sopris]*		✓	Digital image of borehole wall (unitless)	Open face of borehole wall Minimum azimuthal resolution: 1.25 pixel/deg *[Minimum scan width: 0.001 m]*	0.5 m/min	0.001 m	In open rock: lithological characterization; structural orientation (strike direction & dip), fracture aperture at borehole wall

Downhole Geophysical Log *[Manufacturer]*	**Req. Fluid**	**Req. Cent.**	**Logging Unit**	**Radius of Investigation** ***[Vertical resolution]***	**Logging Speed**	**Logging Interval**	**Practical interpretations in open rock**
Acoustic Televiewer *[Advanced Logic Technology/ Mount Sopris]*	✓	✓	Dual images: Traveltime (millisec) Amplitude (unitless)	Open face of borehole wall Minimum azimuthal resolution: 1.25 pixel/deg *[Minimum scan width: 0.001 m]*	0.5 m/min	0.001 m	Limited to fluid filled portion of borehole in open rock: structural orientation (strike direction & dip), fracture aperture at borehole wall
Acoustic Caliper Interpreted from ATV traveltime image	✓	✓	mm	Open face of borehole wall [Caliper resolution: 0.0001 m]	0.5 m/min	0.001 m	Wall roughness, fracture aperture at borehole wall
Fluid Temperature & Conductivity *[Mount Sopris]*	✓		degrees Celcius (°C) ---------- µS/cm calibrated to 25°C	Influenced by surrounding materials [logging interval]	1 m/min	0.01 m	Anomalies due to groundwater flow
Full Waveform Sonic *[Advanced Logic Technology/ Mount Sopris]*	✓	✓	Traveltime (ms)	Influenced by rock quality of borehole wall [0.05 m]	3 m/min	0.05 m	Interpreted P-wave and S-wave velocities in rock surrounding borehole;
Heat Pulse Flowmeter *[Mount Sopris]*	✓	✓	US Gal/min	Within borehole 0.03 USGal/min	Stationary readings	User selected; based on ATV and fluid temp. results	Direction and volume of flow, zones of hydraulic conductivity

Laboratory checks were performed on the fluid temperature/conductivity probe, and orientation systems of the ATV & OTV tools before leaving for the field. Upon arrival at each site, the water level in the borehole was measured using a water level meter. A slug of borehole fluid was drawn from the top of the water column and tested using a calibrated handheld fluid conductivity/temperature probe corrected to 25ºC (Oakton CON 6+ conductivity meter). These values were compared with the values collected by the downhole fluid probe before each run to confirm the values were within 2% of the meter readings.

Downhole data were acquired using a Mount Sopris logging system with a Matrix console and interchangeable downhole probes. A laptop computer recorded the data using the Matrix Logger Software. Corrections for sensor offset and casing stick up were made prior to logging, and logs were recorded relative to ground surface.

The temperature tool was the first instrument lowered into the borehole to avoid disturbing the borehole fluid. A period of 15 - 20 minutes was allowed for the tool to thermally equilibrate in the top of the water column before the downward logging was started.

Following the temperature logging, a downhole video camera was lowered into the borehole to investigate the water clarity (for OTV logging) and the stability of the borehole wall for further logging with the centralized probes. Conditions permitting, televiewers were run, followed by natural gamma, guard resistivity, and full waveform sonic (FWS) tools in any order.

The televiewers were centralized in the borehole using a pair of aluminum, four-arm bowspring centralizers. Decentralization negatively affects the quality of the image (especially for the ATV), so care was taken to ensure the tool was well centered in the borehole prior to recording. Maximum image resolution was used during the logging (288 pts per revolution, or 1.25 pixels/deg, with 0.001 m logging intervals). The image logs were collected from the bottom of the hole upwards, to keep constant tension on the wireline at low logging speeds (<1 m/min). The FWS tool was also centralized and logged upwards.

Once the televiewer and fluid temperature/conductivity logs were reviewed together, intervals for the heat pulse flowmeter testing were selected to bracket visible deviations in the fluid temperature/conductivity logs, and/or presence of open (or partially open) fractures seen in the ATV/OTV images. During heat pulse flowmeter (HPFM) testing, ambient flows (i.e. natural upward/downward gradients in borehole fluid) were not observed in any of the boreholes. Therefore, a Redi-Flo 2 Grundfos pump and controller unit were used to induce upward flow in the borehole. The pump could be lowered to a maximum depth of 75 m, which allowed it to be placed at various depths in the borehole. The flow rate from the pump was monitored every minute on surface using a graded bucket and a stopwatch, while water levels were measured in the borehole using a water-level meter. The flow rate was carefully adjusted in an attempt to equalize the pumping rate with the recharge to eventually achieve no measurable drop in water level during the pumping. The rate was kept below 4 L/min so as not to exceed the HPFM's upper limit of 1.0 USGal/min (3.78 L/min).

To ensure the change in flow rate measured by the tool could be attributed to changes in fracture flow and not to changes in the pumping rate, achieving a constant rate was a very important element of the test. In non-hydraulically conductive boreholes such as these, reaching stability was very difficult and only occurred in F-7 and F-8. In other boreholes where a stable upward flow was not achieved, the measured HPFM results were converted during processing from a volumetric value (L/min), to a

percentage of the total pumping rate measured simultaneously at the surface (L/min) during the downhole flow measurement.

Once the pump was running, (and pump rates stabilized if possible) the test began with the tool positioned at the first depth of interest. Once three heat pulse triggers yielded the same values (±0.08 L/min), the test continued, moving the tool to the next target depth. Five-to-ten minutes were given for the fluid to stabilize after the tool was moved in the borehole. The HPFM testing concluded with final measurements made inside the casing to identify whether the contact between casing and bedrock was sealed.

Composite log figures and tables containing the results of the flowmeter testing can be found in Appendices II and III, respectively.

3.0 Data Processing

Data were imported into WellCAD (V 5.0) processing software and displayed as a suite of logs for each borehole (see Appendix B). Natural gamma, resistivity, and fluid/HPFM logs did not require additional processing. However, analyses were required on the televiewer and full waveform sonic logs, and are described herein.

3.1 Optical and Acoustic Televiewer logs (Structural Orientations)

Optical and acoustic televiewer images were imported into the WellCAD image processing module and were immediately oriented to magnetic north. The color palate of the acoustic amplitudes and traveltimes of the ATV logs could be adjusted to enhance the on-screen appearance of structural features.

Before beginning image interpretation, the borehole diameter must be accurately known, as this value influences the azimuth and dip direction of the interpreted structural features. A **360° acoustic caliper** log was calculated using the traveltime data collected during the ATV logging, and a fluid velocity of 1427 m/s (a value which takes into account the measured fluid temperature). Smooth walls in the diamond drilled boreholes resulted in high amplitude reflections for caliper calculations. However, fractured intervals, and the downhole hammer drilling methods used in boreholes F-10 through F-13, created rough borehole walls where acoustic signal could be lost or attenuated. When signal is lost, the only acoustic reflector detected by the tool is the first multiple of the reflected acoustic signal on the tool's acoustic window. This creates an erroneous early arrival time which interferes with the caliper calculation. Therefore, where present, these arrival times were removed from the traveltime dataset using a filter. The software calculates minimum, maximum, and average borehole diameters, which were verified against the known diameter of the casing (96 or 152 mm). Having min, max, and average caliper logs enhances the interpretation of structural features, as a continuously open fracture will increase in diameter in both the minimum and maximum logs.

A structural column linked to the average caliper log was created and laid over the televiewer logs. The unwrapped images of the inside of the borehole wall cause planar dipping features appear as sinusoids. Sinusoids were fit to these features using the WellCAD software and structures (bedding, joint, etc…) were interpreted and classified according to Table 4. "Open" features could be further

classified as “flowing” based on the presence of a deviation in the fluid logs at that depth. The flowing feature class is a sub-category of broken or open features.

Dip angles of the structures were then corrected for minor borehole tilt (1-5° from vertical) as measured by the televiewer’s accelerometers. The structures were finally exported relative to magnetic north for stereogram interpretation.

Table 4. Structural classification for the St-Édouard project.

Structure Type	Structure Sub-type	Structure Code*	Tadpoles (non-flowing)	Tadpoles (flowing)
Broken Zone	No apparent structure (eg. fault zones, washouts)	BZ		
	Fractured beds (eg. network of vertically fractured beds)	BZ - FB		
Open Features	Open bedding planes	OB		
	Open continuous joints	OC		
	Open discontinuous joints	OD		
Closed Features	Closed bedding / foliation planes	CB		–
	Closed / infilled joints	CJ		–
	Offset joints	OfJ		–

* Codes for structures which are interpreted as flowing are followed by a “-F”.

Data were subsequently corrected for declination for stereogram presentation using SpheriStat software (Version 3.1) produced by Pangea Scientific. Planar structural features were plotted as points on stereograms, representing poles after plane projection on the lower hemisphere of an equal-area Schmidt diagram.

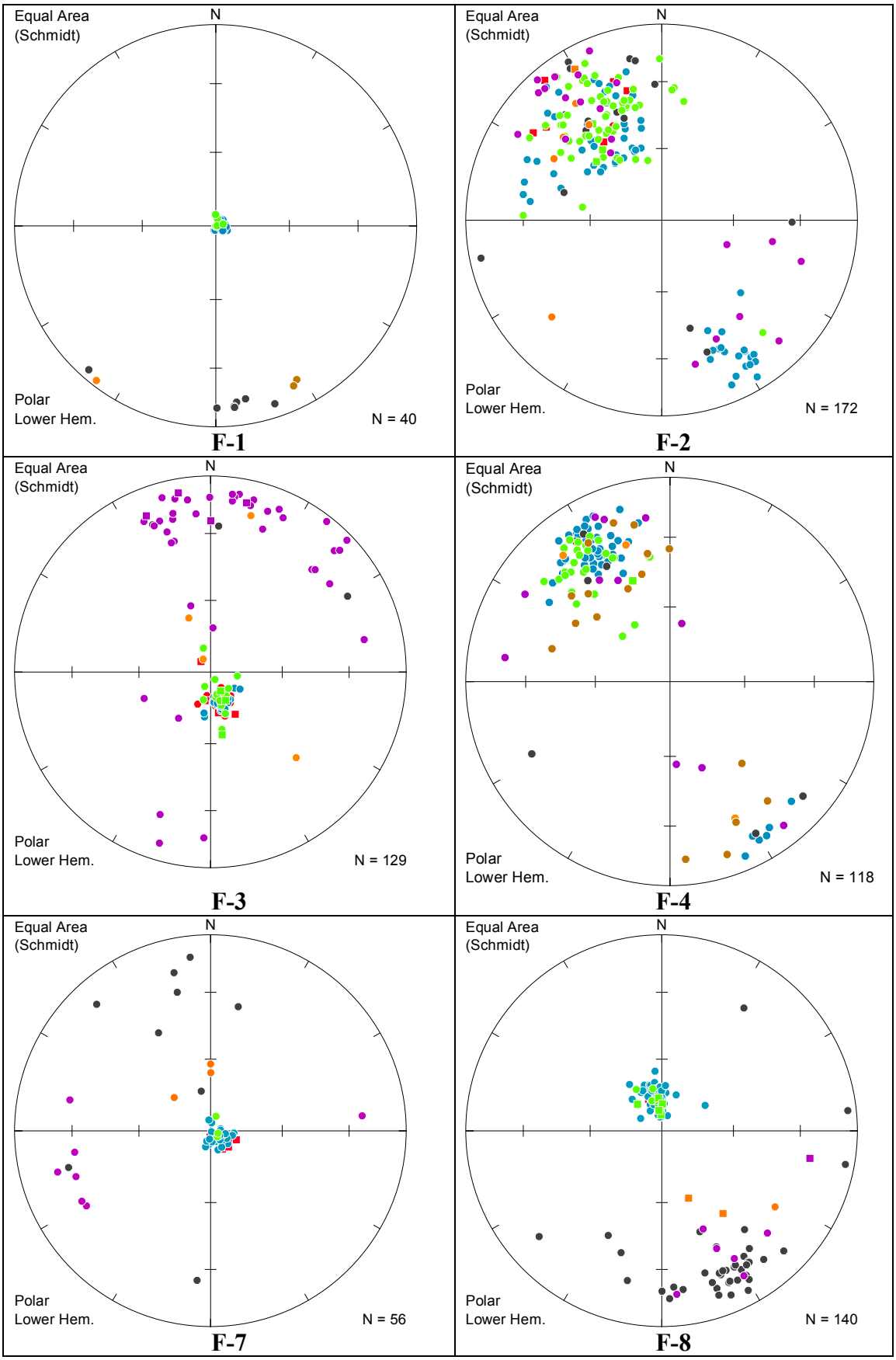
Equal Area
(Schmidt)
N
Polar
Lower Hem.
N = 40
F-1
Equal Area
(Schmidt)
N
Polar
Lower Hem.
N = 172
F-2
Equal Area
(Schmidt)
N
Polar
Lower Hem.
N = 129
F-3
Equal Area
(Schmidt)
N
Polar
Lower Hem.
N = 118
F-4
Equal Area
(Schmidt)
N
Polar
Lower Hem.
N = 56
F-7
Equal Area
(Schmidt)
N
Polar
Lower Hem.
N = 140
F-8

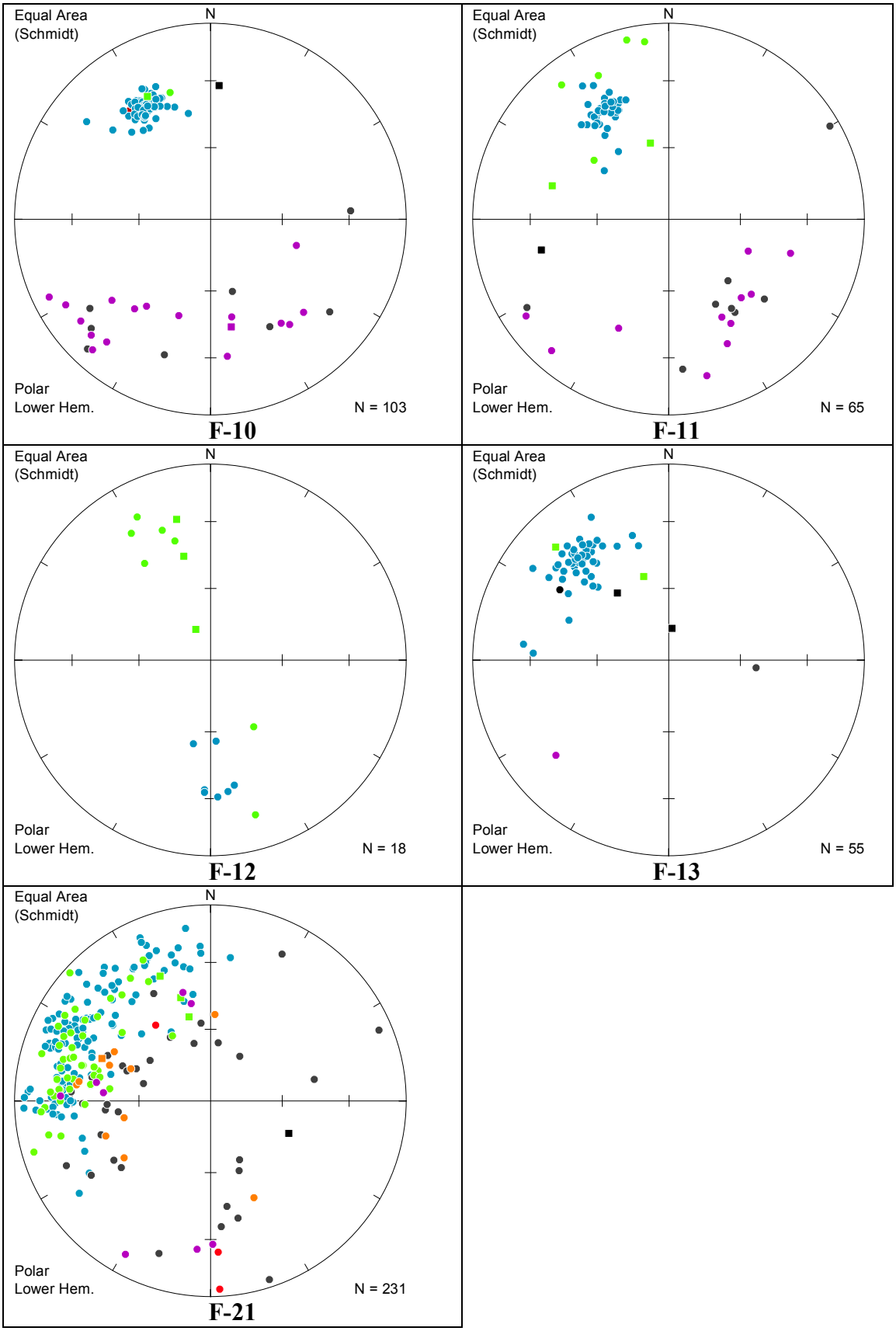

Figure 2 – Stereonets based on structures interpreted from optical and acoustic televiewer logs. Poles are color-coded based on Table 4.

3.2 Full waveform sonic logs (P- and S-wave velocities)

Velocities were computed using the WellCAD full waveform sonic processing module. P-wave velocities were computed from transit times using a first arrival picking algorithm on all three receivers. The algorithm returns a well log containing the first arrival intercept times (Figure 3). The transit time between two receivers (generally Rx 1 and Rx2) divided into the distance between them (20 cm) gives the P-wave velocity for that interval.

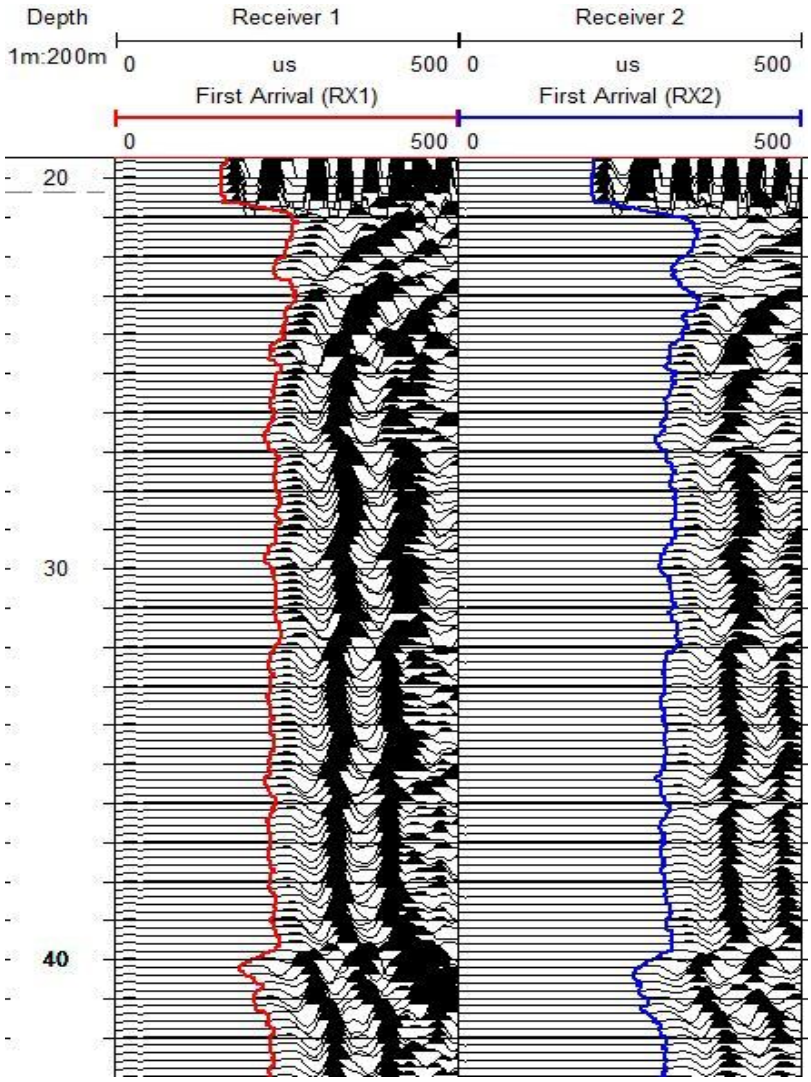

Figure 3 – Waveforms (trimmed at 500 µs) from Receivers 1 and 2 showing first arrival picks. Steel casing ends at 21 m depth. Transit times between the two receivers are used to calculate P-wave interval velocities ('first arrival method').

A velocity analysis process called 'semblance processing' which looks for similarities in waveforms across the three receiver array was used to determine the slowness (µs/m) of P and S waves. For each depth, the algorithm starts with an assumed slowness and computes a coherence value for all the receiver responses. Figure 4 shows a sample coherence plot from borehole F-1 with slowness logs identified for P- and S-waves. Velocity logs in m/s can then be computed from slowness logs (µs/m).

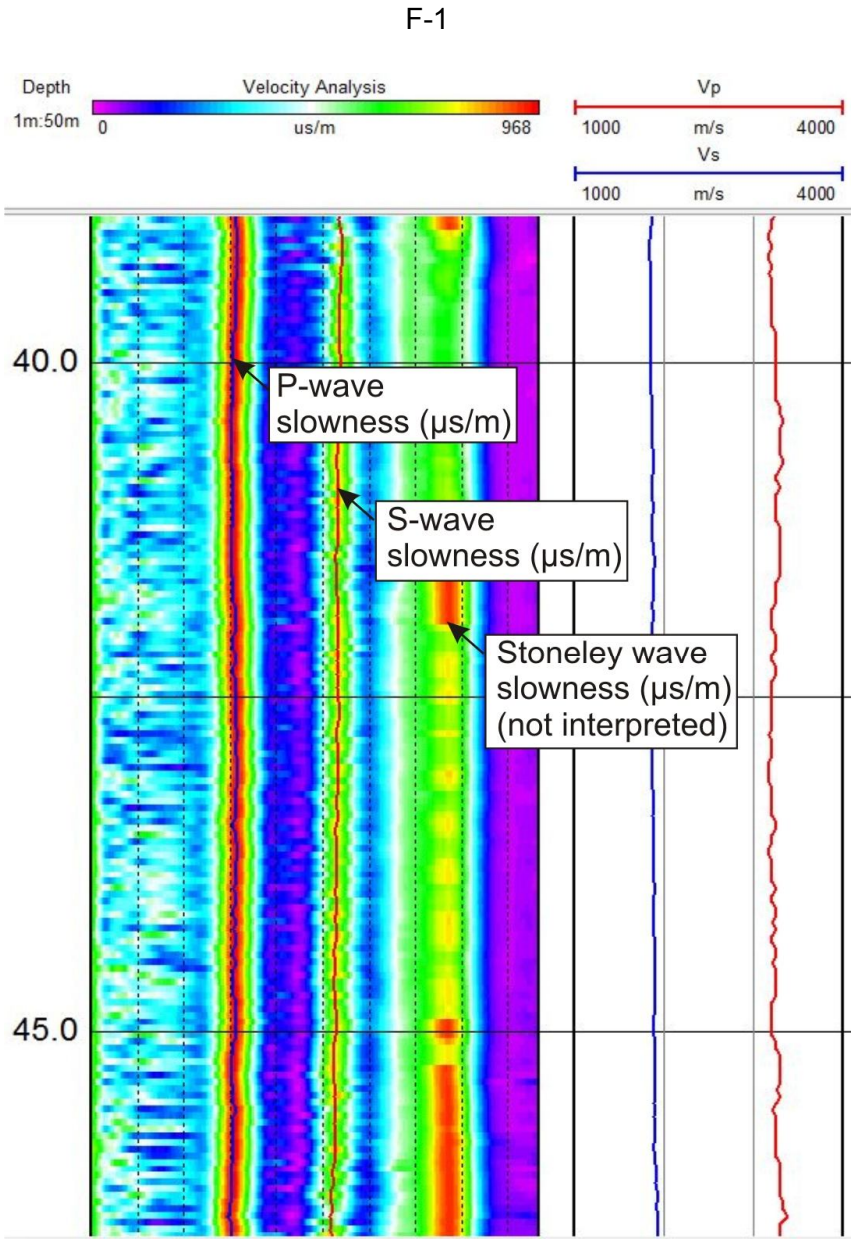

Figure 4 – Coherence log from semblance processing in F-1 for P- and S-wave slownesses (µs/m). Slowness logs can then be converted to velocity logs (m/s).

A quality check on the velocity analyses was performed by superimposing the P-wave velocities calculated using the first arrival method with the semblance processing techniques. They were routinely within 5% of one another, indicating the semblance processing was correctly identifying the peak coherence values, giving increased confidence in the S-wave velocity analyses.

Within intervals of fractured rock, common in the upper 50 metres, the signal could be slowed or even lost. Figure 5 provides an example of the velocity analyses in competent and fractured bedrock, shown alongside the acoustic televiewer log. The ATV log was an important element of the velocity analyses, providing a high resolution image of the borehole wall to better understand the signal behavior.

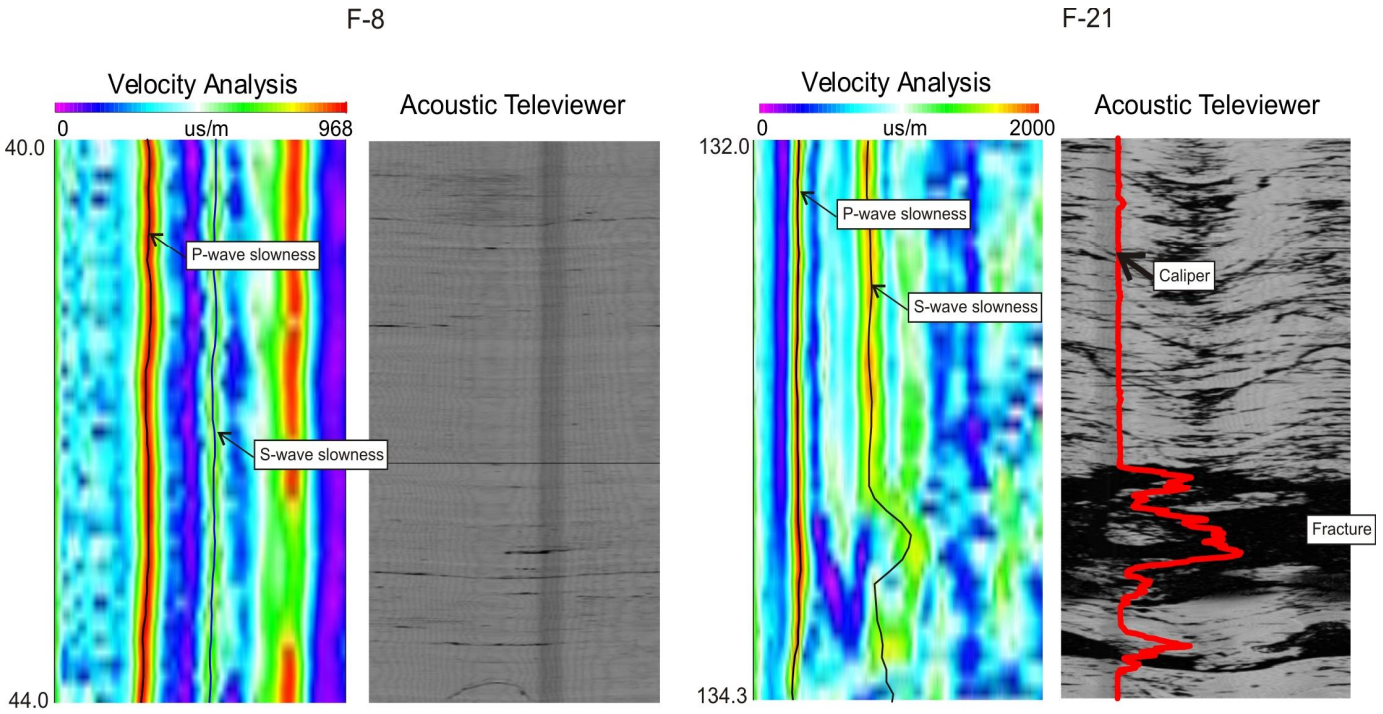

Figure 5 – Comparison of velocity analyses within an unfractured (F-8) and fractured (F-21) segment of the borehole wall. Within the fracture in F-21, there is a reduction of signal coherency and slowing of the S-wave traveltime.

4.0 Interpretation

4.1 Lithological Logs

The primary logs used to interpret lithological variation were the resistivity and natural gamma logs, with the optical televiewer providing digital borehole wall imagery where fluid was clear. Subtle grainsize variation was most effectively detected by the resistivity tool. Examples are shown in Figure 6 where the resistivity log identifies intervals (10^{+}m) of overall lower resistivity (or higher conductivity) versus the overlying/underlying formation, indicating a subtle increase in finer grainsize content (e.g. shale), which was not evident in the natural gamma logs alone.

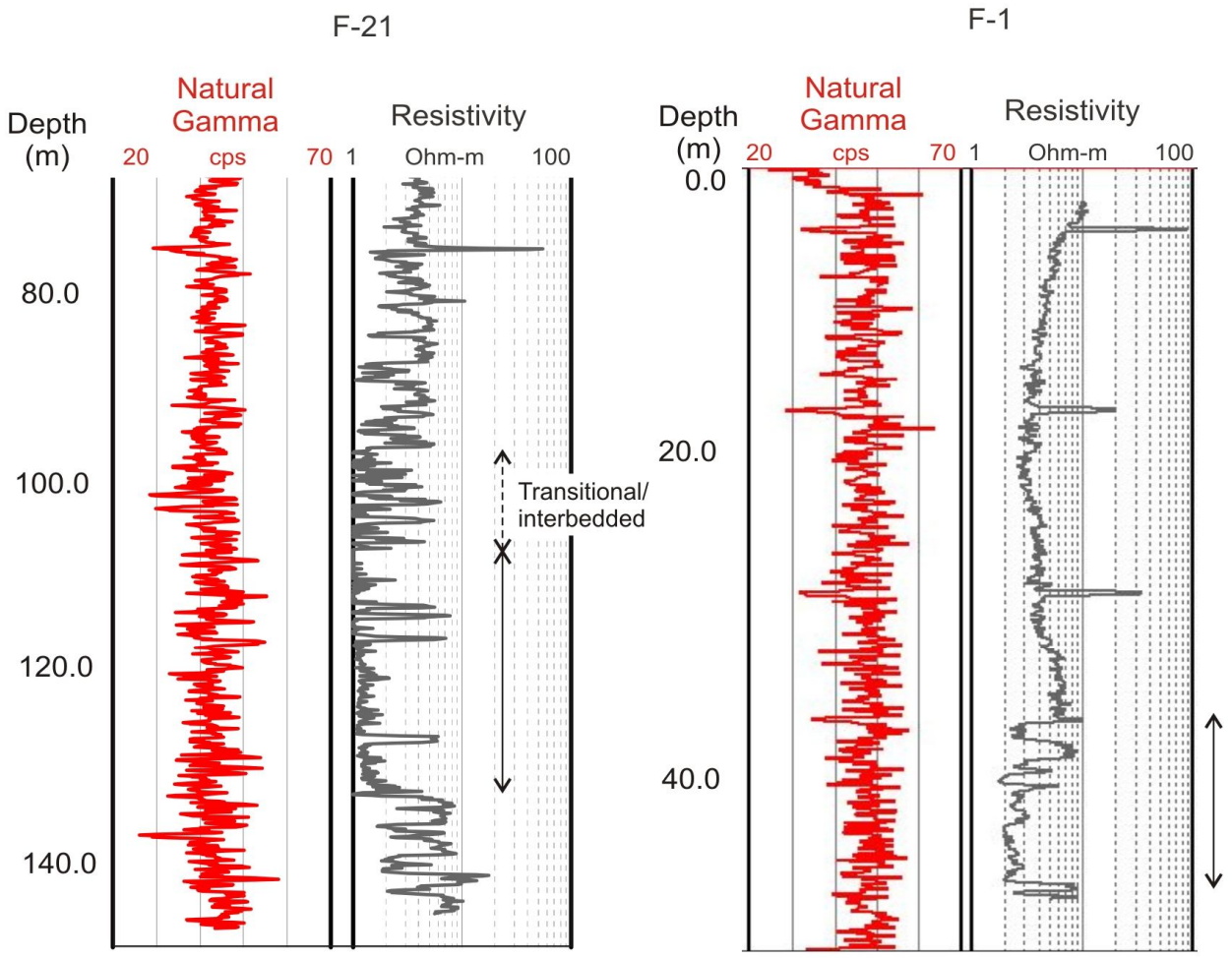

Figure 6 – Intervals of decreased resistivity (shown with arrows) indicate subtle downhole geological variation in fine grained bedrock (shalier rock), not evident in the natural gamma log.

On a centimetre-scale, the resistivity log also identified cemented siltstone interbeds in a predominantly shale bedrock. An example is shown in Figure 7 where increases in resistivity were confirmed by core observation to be siltstones.

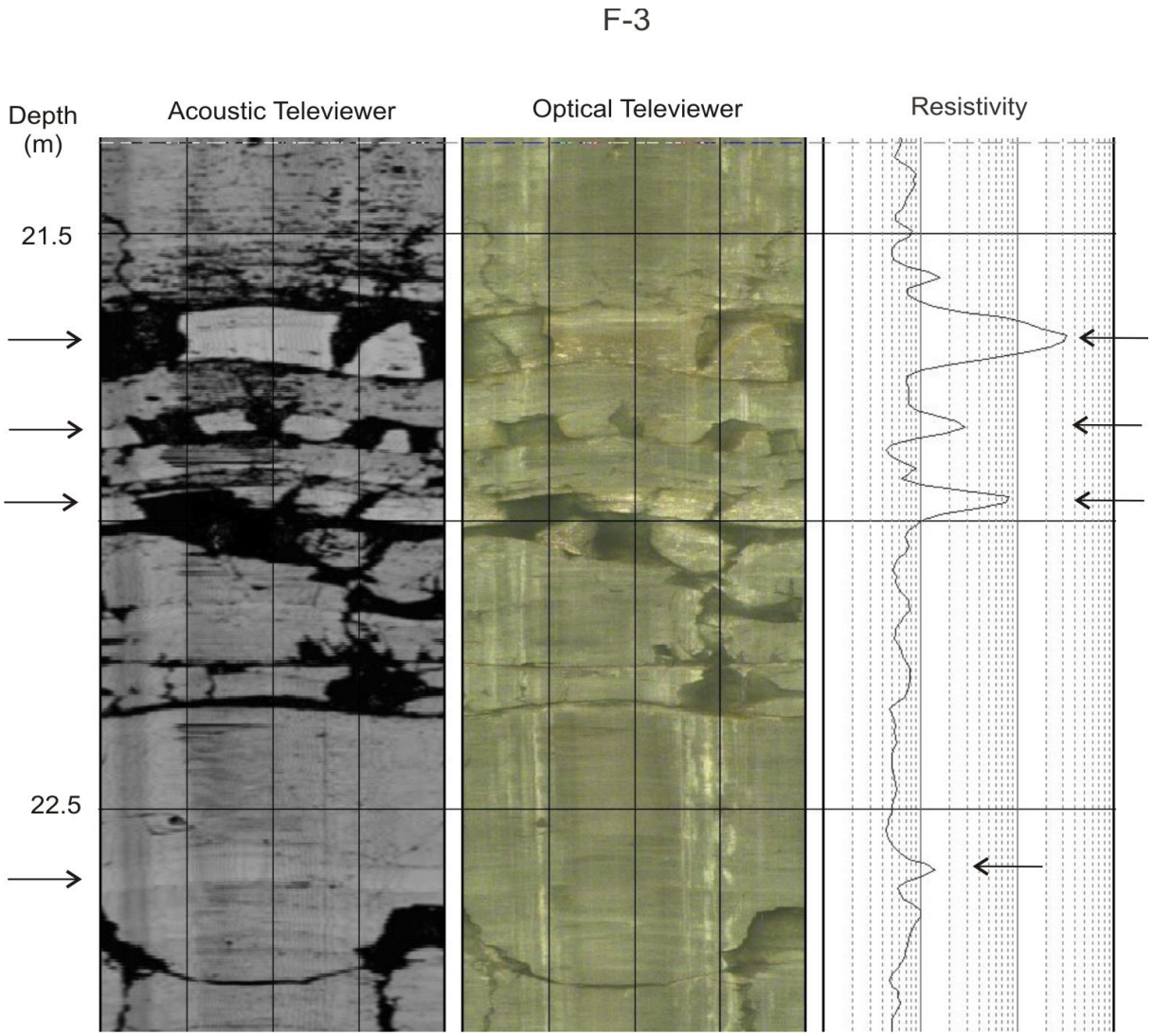

Figure 7 – Arrows indicate sub-horizontal siltstone beds (containing vertical fractures), which are apparent in the resistivity logs.

An example is presented in Figure 8 where a drop in gamma counts and an increase in velocity, resistivity, and acoustic reflectance coincides with highly cemented siltstone beds. These beds were most prominent in borehole F-1, but were also observed to a lesser extent in F-2, -3, -8, -10, and -21.

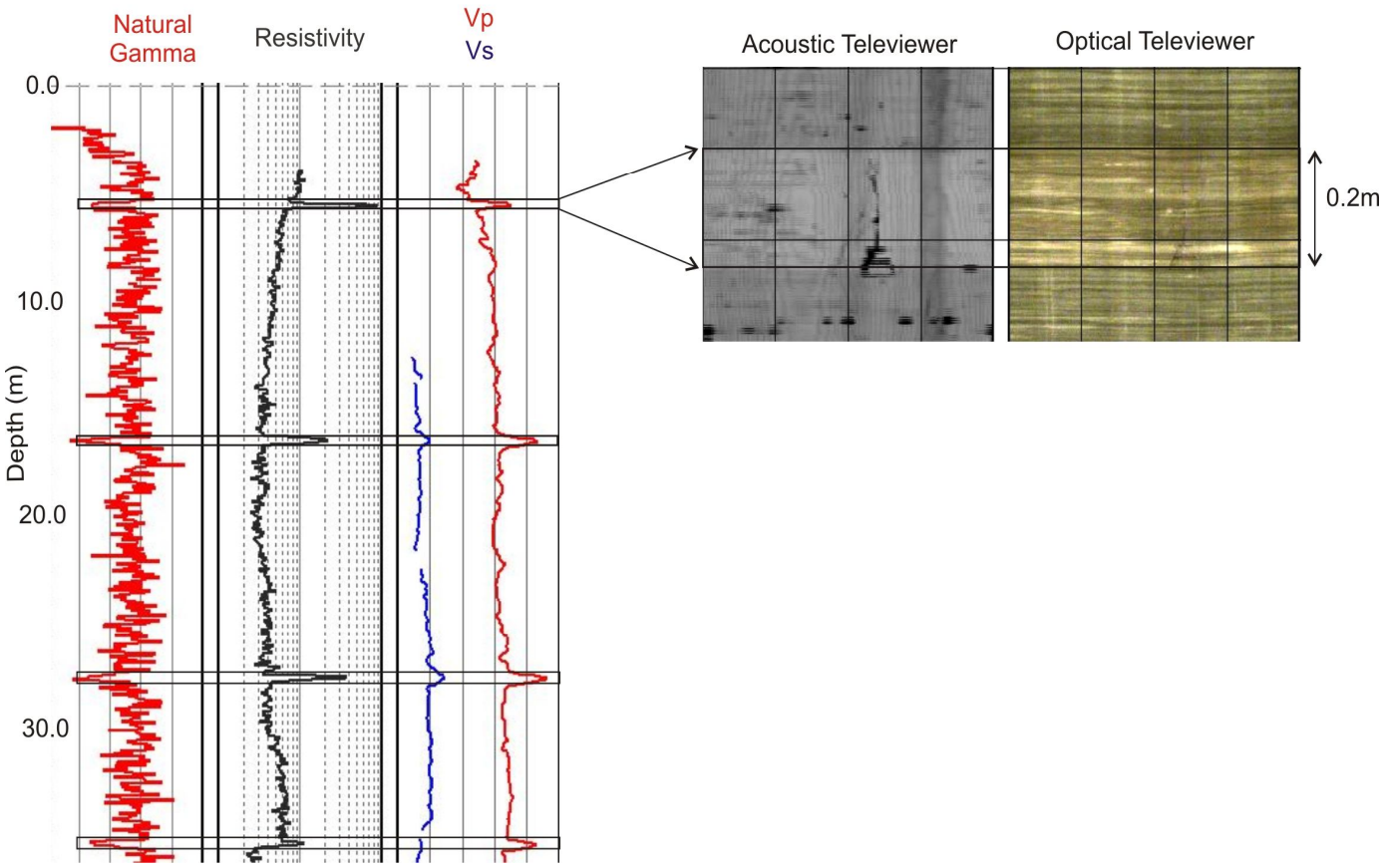

Figure 8 – In F-1, four intervals were identified as having reduced gamma counts and elevated resistivity and velocity. Televiewer images also indicate an increased acoustic reflectance and a change in the color of the rock. These intervals are interpreted as highly cemented; core observation indicates these are calcareous siltstone beds.

Resistivity anomalies could also be indicative of structural anomalies. Figure 9 shows an example of a highly folded shale interval which has been fractured and recalcified within a brecciated zone in borehole F-21. A photograph of a 0.7 m-long segment of core from this brecciated interval is also shown. The televiewer image allows for a measurement of the structural orientation *in situ*, which is often lost in brecciated core intervals.

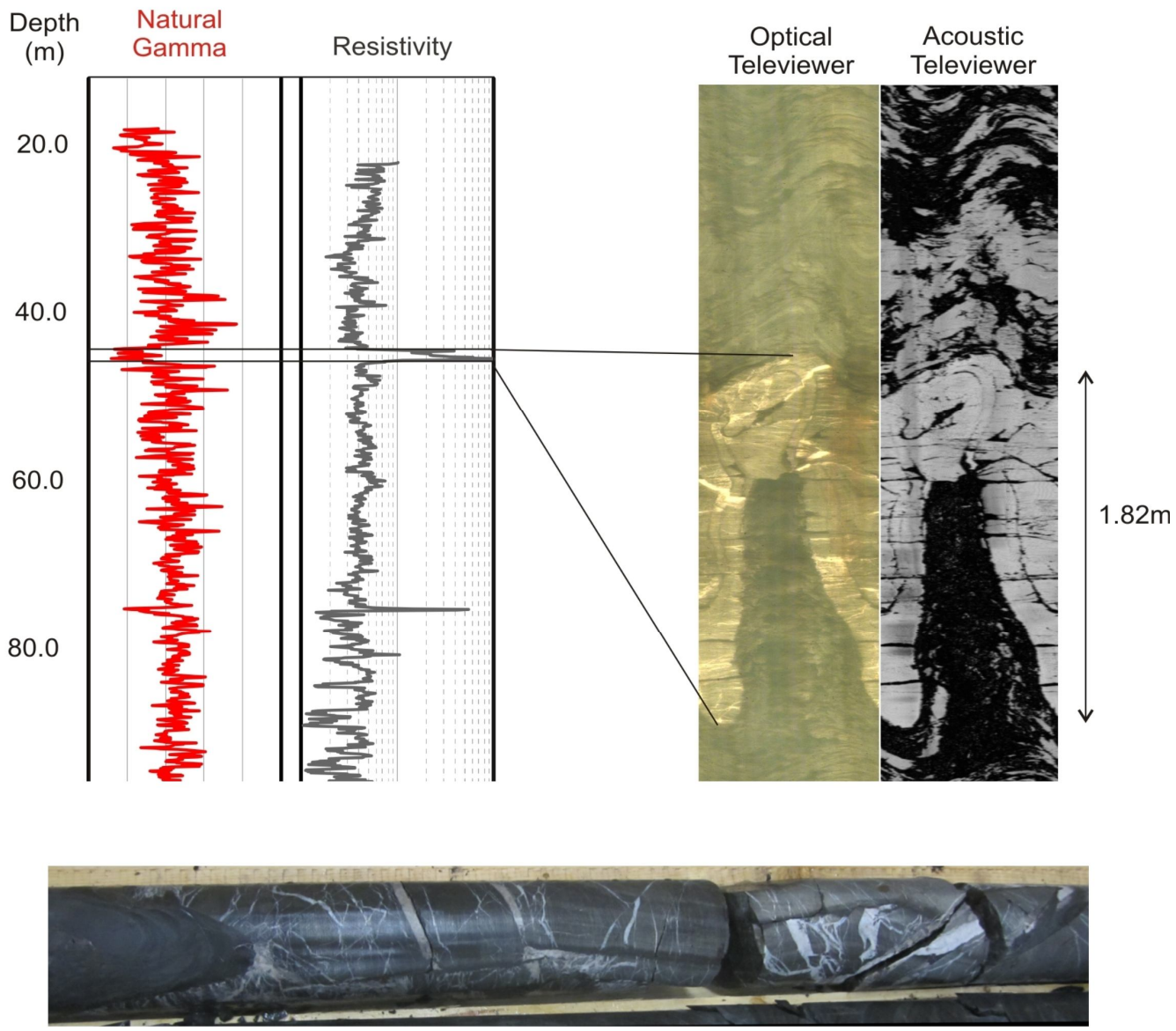

Figure 9 – Decrease in gamma counts and increase in resistivity correlate with a folded and recalcified bed within a brecciated zone, as seen in the OTV image. Shown below the logs is a 0.7 m length of core, photographed at the same depth.

4.2. Structural / Geomechanical Logs

4.2.1 Preliminary structural log observations

Boreholes in the **autochthonous domain** (F-1,-3,-7,-8) predominantly exhibit flat-lying bedding (max. dip angles around 20°). Most of the open fractures intersected by the boreholes are contained in this sub-horizontal feature set. High angled fractures were occasionally observed in shale formations (and were sometimes calcite-filled), but most high angle features were seen in the sandstone/siltstone beds (see Figure 7). Some centimeter-scale bed offsets were observed along some fracture planes as shown

in Figure 10 (F-1), but this is not a general trend observed in the area, as the St. Lawrence platform rocks are not affected by a high degree of deformation.

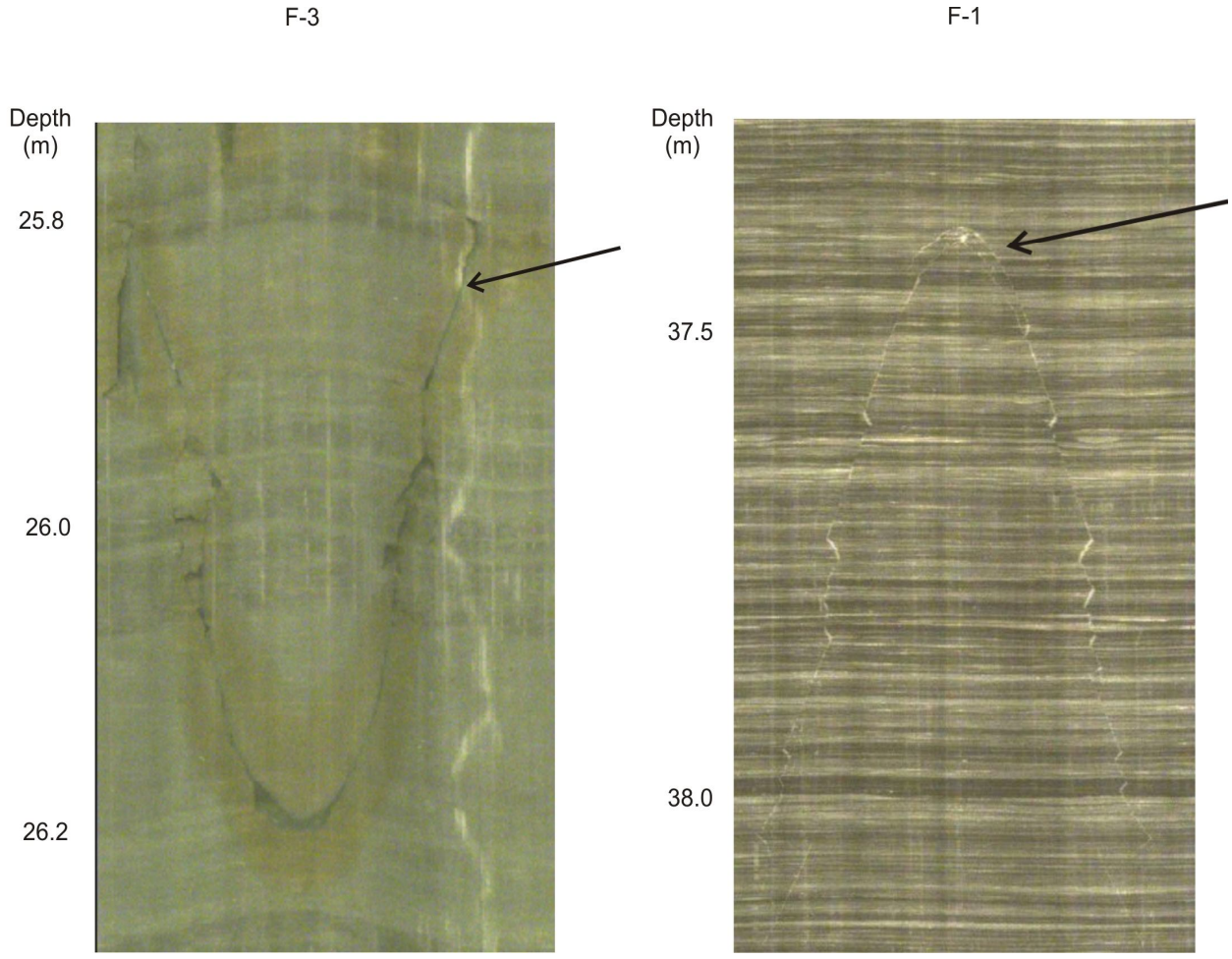

Figure 10 – Unwrapped optical televiewer images showing sub-horizontal bedding in boreholes F-3 and F-1. In F-3, the arrow indicates a high angle dipping open fracture (note iron staining), and in F-1, a steeply dipping fracture healed with calcite shows minor bed offsets (approx. 0.5 cm). In both cases, bedrock is shale.

All the structural features interpreted in the **parautochthonous and allochthonous domains** (F-2, -4, -10, -11, -12, -13, -21) exhibit the same pattern: a NNE-trending strike direction of the bedding planes, consistent with the faults and associated fold orientations of the Appalachian frontal zone. As observed in the autochthonous zone, most of the open fractures are contained in the beddings planes. Fractures oriented orthogonally to the bedding were also observed in most of the wells. Locally, some mesoscale (centimetre to metre-scale) fault planes were observed (Figure 11).

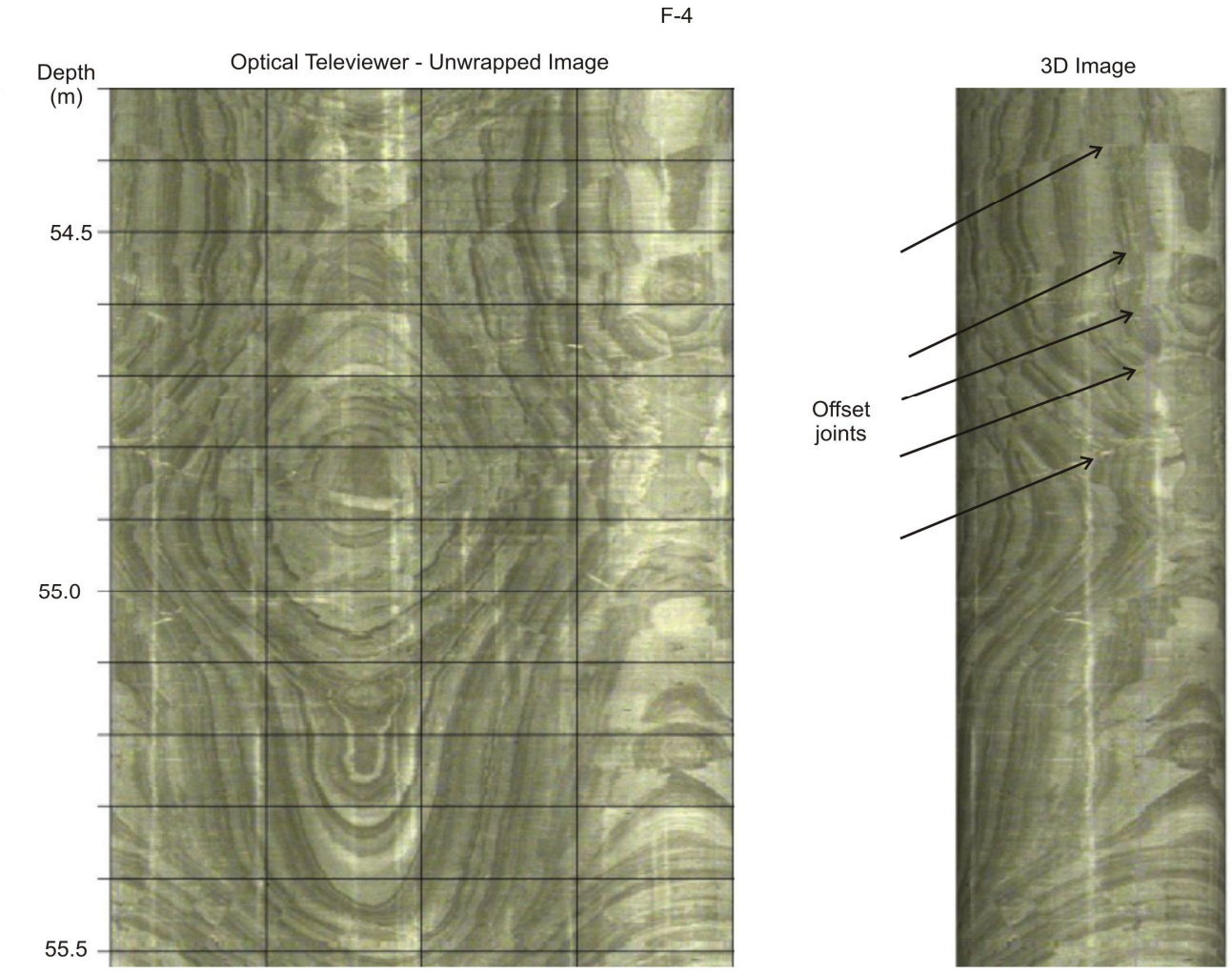

Figure 11 – Optical televiewer image from borehole F-4 showing a fold and a set of joints offset by up to 2.5 cm.

4.2.2 Sonic logs

Summary results of the sonic log interpretation are presented in Figure 12. Almost all of the boreholes were affected by moderate to significant fracturing (or even shearing in the case of F-2 and F-21) in the upper 25 m of the well, often causing a complete loss of S-wave signal within these intervals. P-wave velocities were calculated to be 3200 ± 350 m/s (1σ) and S-wave velocities were calculated as 1850 ± 140 m/s (1σ). The low end of the velocity range is attributed to zones weakened by fractures and shear zones (as shown in Figure 5); occasional zones strengthened by cementation or calcification formed the highest end of the range (e.g. F-1, see Figure 8).

A plot of the Vp:Vs ratio indicates the relationship ranges primarily between 1.5 and 2 within the upper 50 m of the ground surface; this ratio also holds for F-21 up to 150 m depth. In sheared or heavily fractured intervals (F-2 and F-21), this ratio generally exceeds 2.

An average Poisson's ratio was calculated to be 0.25 ± 0.06 (1σ) which is in agreement with other measured values in this region (e.g. Molgat et al., 2011) and in the Utica shale in Ohio (Daniels et al.,

2011). In St-Édouard, the standard deviation in these calculations is tied to the variability in P- and S-wave velocities where fractured bedrock is present in the near surface.

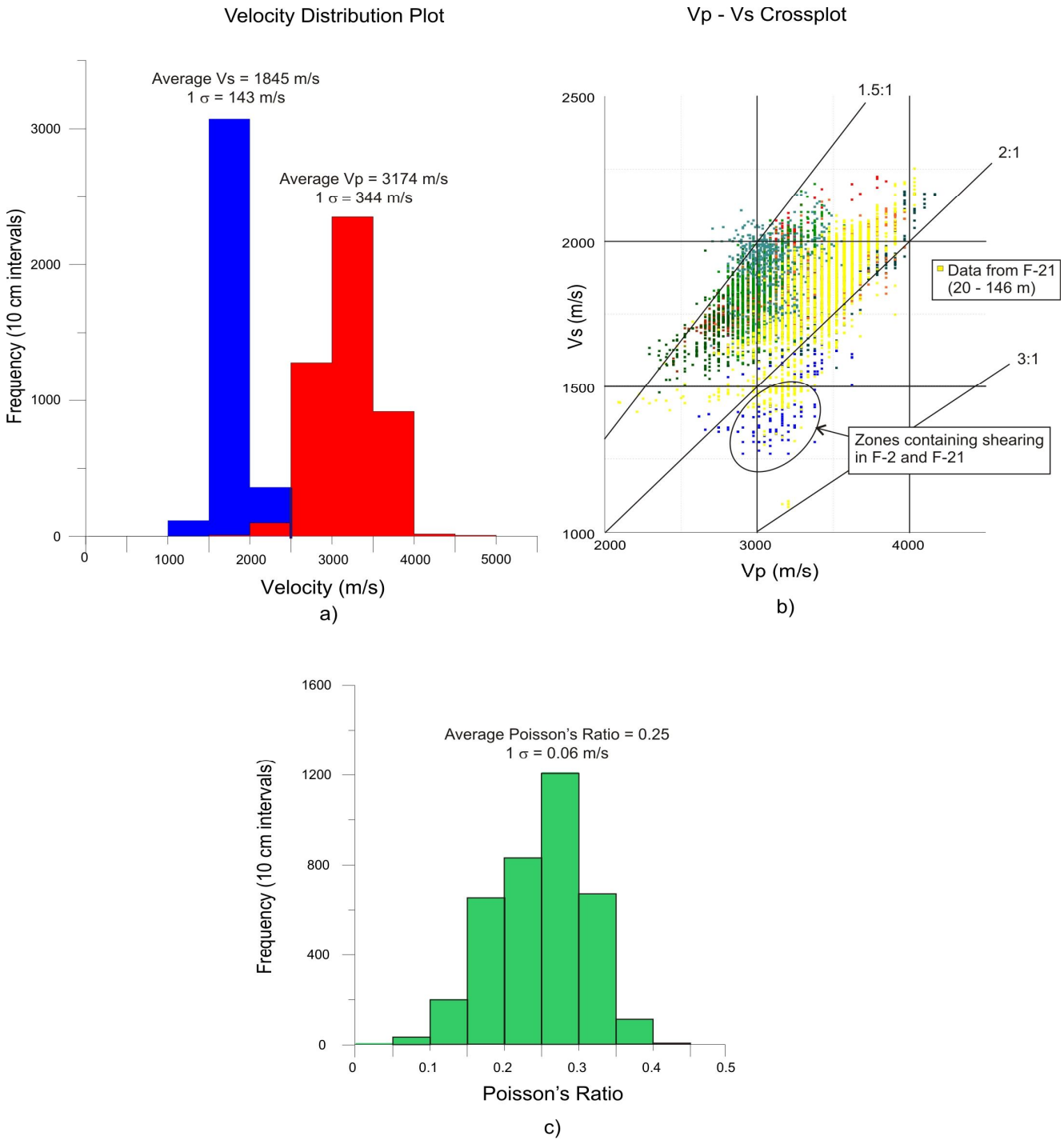

Figure 12 – Results of sonic log interpretation (resampled at 10 cm intervals) from all 11 boreholes. a) Velocity distribution of P- and S-wave velocities. b) Crossplot of Vp:Vs indicating the majority of the ratios fall between 1.5 – 2, even within the deepest borehole, F-21. Values > 2 occur within sheared zones. c) Distribution of Poisson's ratio, calculated from Vp and Vs. The wide range in values is caused by the fractured nature of the bedrock in the near surface.

The sonic traveltimes and Poisson's ratios were incorporated into a comparative study of the deeper formation to determine whether geomechanical properties of the rock capping the Utica shale at depth can be extrapolated to the surface (Séjourné, 2015). Séjourné (2015) found that sonic log data (150 – 700 m) extracted from nearby industry well datasets shows a consistent relationship with shallow GSC boreholes F-21 and F-8. In the remaining F-series boreholes, the presence of fractured zones in the near surface complicates this relationship. There is also a consistency in the Poisson's ratio values calculated from deep and shallow datasets, ranging between approximately 0.2 and 0.35.

4.3 Hydrogeophysical Logs

The borehole fluid temperatures deemed most representative of near surface conditions were measured in boreholes F-2 and F-4, which were drilled in 2013 but relogged in 2014, allowing for a long period of stabilization. Fluid temperatures ranged between 6.5 – 6.8 ºC. All other boreholes were logged one week to one month after the drilling completion, and tended to be 1 – 2 ºC warmer.

One of the key goals of the hydrogeophysical logging was to identify fractures transmitting fluid into/out of the boreholes. Anomalies in the fluid temperature and conductivity logs acquired in the undisturbed borehole fluid indicated that fluid was entering the boreholes where fractures could be seen in the televiewer images. An example is shown in Figure 13 where fresher, less conductive, groundwater was flowing into the fluid column filled with silty fines from recent drilling, leading to an upward decrease in fluid conductivity. Based on the results of these logs, a list of recommended depths for geochemical testing was delivered in the field for immediate sampling.

In general, the borehole fluid conductivities were < 2000 µS/cm. It is difficult to know whether these values are representative of the near surface groundwater conductivities, as all of the boreholes contained residual fines from the drilling and some were too cloudy to image with the OTV. However, conductivities in borehole F-4 after a one year settlement period ranged between 1400 – 1700 µS/cm, suggesting these values reflect natural groundwater conditions in some locations. Of note, were unusually elevated fluid conductivities encountered in the base of F-21 (at ~134 m: reaching a max of 3000 µS/cm), F-1 (at ~36.5 m: 7000 µS/cm), and along the entire length of borehole in F-7 (10,000-13,000 µS/cm). Geochemical values obtained with a handheld multiparameter probe through low-yield pumping at depths identified by this work confirm these values. Conductivities for these 11 wells vary from 190 to 9560 µS/cm with a median of 862 µS/cm.

Results from the follow-up flow meter tests are presented in bar chart form on the log suites in Appendix B and in detailed tables in Appendix C. In all boreholes, vertical fluid movement between fractures was not detected under ambient conditions using the HPFM, which has a lower detection limit of 0.1 L/min. Therefore, HPFM tests were run under pumped conditions to identify the relative contribution of each fracture to the overall volume pumped out of the well. In general, the boreholes did not contain many hydraulically conductive fractures, and a stable water level could not be reached during pumping except in boreholes F-7 and F-8 (at low rates of 2 and 4 L/min, respectively).

F-2

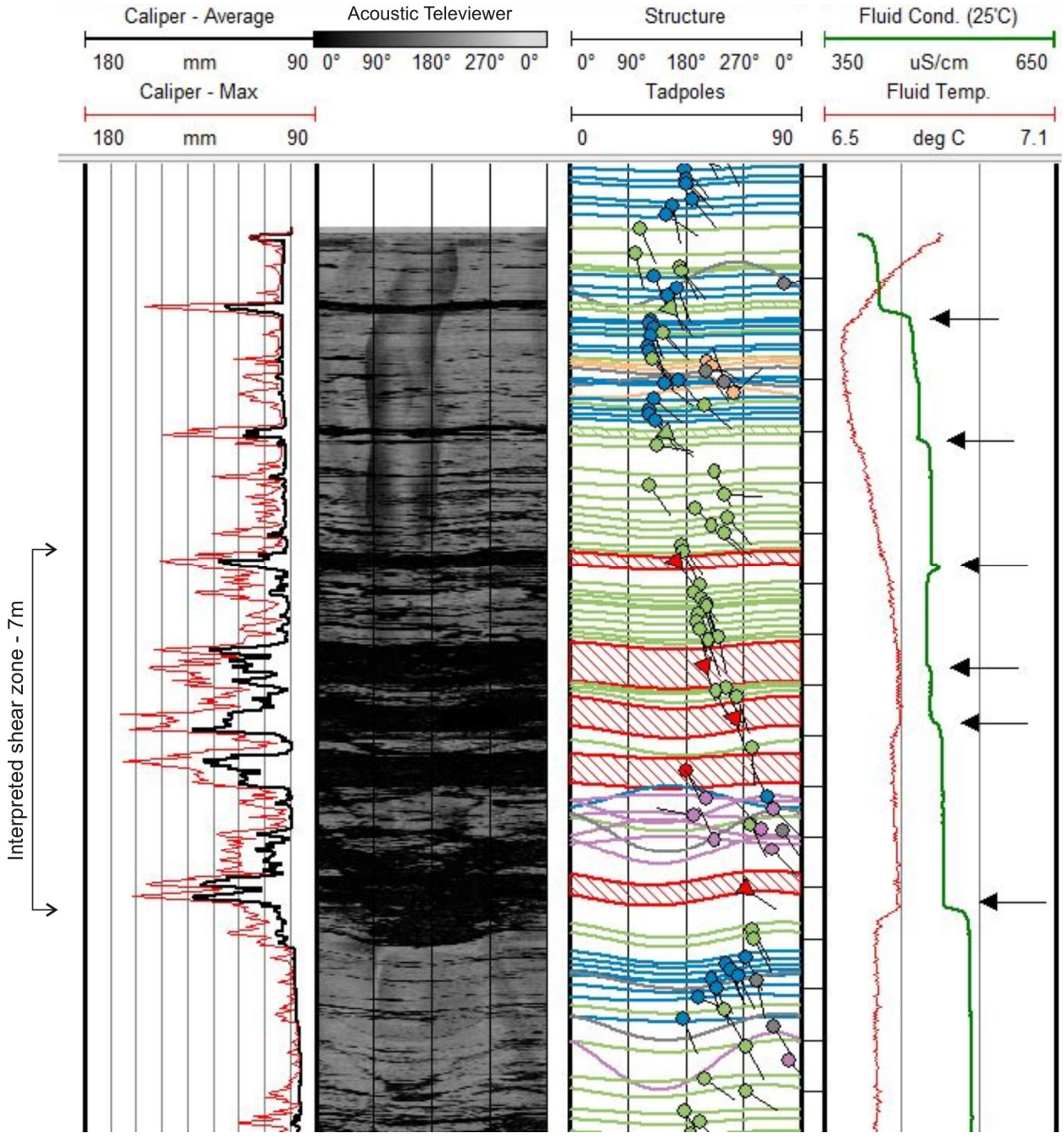

Figure 13 –The locations of borehole wall fractures in F-2 are identified using the caliper and acoustic televiewer image. Anomalies in the fluid logs, identified with an arrow, indicate the features interpreted to be transmitting groundwater which require follow up HPFM testing. This information allows for structural features to be assigned as "Flowing" or "Non-Flowing". Colors of the structures and tadpoles are based on Table 4.

During the HPFM test in F-8, fluid pumped to surface was sampled regularly with a calibrated hand-held fluid conductivity/temperature meter. With the pump lowered to 3.3 m, the temperatures ranged between 9.5 - 10 ºC. Over the first 30 minutes of pumping as the downhole water level stabilized, temperatures dropped from 9.9 to 9.6 ºC and the fluid conductivities dropped slightly from 414 to 408

µS/cm. After an hour of pumping, these values were interpreted the represent the local near surface groundwater conditions in this well. As stable groundwater temperatures in the region were found to range between 6.5 and 7 ºC, the near-surface temperatures measured in F-8 are interpreted to be representative of warmer surface waters which have reached the fractured bedrock.

Finally, gas was only observed bubbling at the water surface in borehole F-1 immediately after drilling. In most boreholes during the flow meter pumping tests, bubbles could be seen in the clear tubing as gas dissolved in the borehole fluid depressurized as it rose to surface.

5.0 Conclusions

A high-resolution geophysical dataset has been collected in 11 boreholes in the St-Édouard-de-Lotbinière, QC, area to support a GSC project studying the potential impacts of shale gas activities on shallow aquifers. The boreholes ranged in depth from 30 to 147 m, and were drilled and geophysically logged in two phases between September 2013 and November 2014.

Lithological variability between shale and siltstone beds was best identified by the resistivity logs. The presence of cemented siltstones, and of calcified beds in sheared or brecciated zones, was also well indicated by a combination of the resistivity and full waveform sonic (velocity) logs. The optical televiewer logs provided high-resolution (mm-scale) digital color images of the inside of the borehole wall. Observation of geological variation at the bed scale was important, as the majority of the fractures were found to be bedding-parallel.

Structurally, bedding orientations measured from the televiewer logs are consistent with the orientation of the regional folds and fault systems. In the autochthonous domain (boreholes F-1, -3, -7, and -8), bedding was horizontal to sub-horizontal (dip angle <20º). Locally, high angle dipping joints and fractures were observed in most of these wells. The structural features interpreted in the parautochthonous and allochthonous domains (boreholes F-2, -4, -10, -11, -12, -13, and -21) exhibit a NNE-trending strike direction of the bedding planes, consistent with the faults and associated fold orientations of the Appalachian frontal zone. In future work, these televiewer data will be analysed with the outcrop measurements and deep industry formation microimager (FMI) orientation data to assess structural continuity (or lack thereof) from depth (~700 m) to surface.

Geomechanically, the sonic tool provided a quick and accurate method for measuring downhole P- and S-wave velocities, and worked equally well in diamond drill and hammer drilled holes. Using first arrival and semblance processing techniques, average P-wave velocities were measured at 3200 ± 350 m/s (1σ), and S-wave velocities were 1850 ± 140 m/s. From the velocity logs, the average Poisson's ratio was calculated to be 0.25 ± 0.06 (1σ) - in agreement with other measurements of shales and siltstones of the region. The presence of fractures in the near surface (especially common in the upper 25 m) led to frequent low velocity intervals, causing variability in the calculated Poisson's ratio. Despite these near-surface fractures, Séjourné's (2015) analyses of industry sonic logs from nearby boreholes ranging in depth from 150 – 700 m indicate there is a consistent relationship in velocity and Poisson`s ratio between the traveltimes measured in some of the near surface boreholes (where rock is relatively unfractured, e.g. F-8, F-21) and the deep industry boreholes.

Fluid and televiewer logs were together used to quickly identify the depths of fractures transmitting fluid, allowing for on-site recommendations of fluid sampling depths for geochemistry analyses. During follow-up HPFM testing, natural vertical flow was not detected in any of the boreholes. Even under pumped conditions, all boreholes were relatively tight, except for F-7 and F-8 where water levels stabilized during pumping tests at rates between 2 and 4 L/min. Fractures which did transmit small volumes of fluid under pumped conditions in all the wells were predominantly found to be horizontal or sub horizontal (bedding-parallel).

Fluid temperatures after a year-long period of settlement range between 6.5 – 7.0 °C (F-2, F-4). However, elevated fluid temperatures measured using a hand held fluid temperature/conductivity meter in F-8 after an hour of pumping indicated much warmer temperatures near the bedrock/soil interface (>9 °C).

Results from these borehole geophysical surveys provide an important link between the properties of the deeper rock mass (150 m – 700 m) and observations of the bedrock in outcrop. Work is currently underway to compare all three datasets to assess potential continuity of geomechanical and structural features at various depths. Results of these studies will assist in providing recommendations for the protection of near-surface groundwater from future potential energy resource extraction at depth.

Acknowledgements

The authors wish to acknowledge Tim Cartwright, Kevin Brewer, Xavier Malet and Jean-Marc Ballard for their work in the field during the downhole logging. With thanks to André Pugin, Mathieu Duchesne, and Stephan Séjourné for their discussions and reviews of the sonic data. With thanks to Christine Rivard for her critical review of this text, and to Denis Lavoie for his contributions to the geological context.

Funding for this work was made possible through the Environmental geoscience Program of Natural Resources Canada.

References

Belt, E.S., Riva, J. and Bussières, L., 1979. Revision and correlation of late Middle Ordovician stratigraphy northeast of Quebec City. Canadian Journal of Earth Sciences, 16(7): 1467-1483.

Castonguay, S., Dietrich, J., Shinduke, R. and Laliberté, J.-Y., 2006. Nouveau regard sur l'architecture de la Plate-forme du Saint-Laurent et des Appalaches du sud du Québec par le retraitement des profils de sismique réflexion M-2001, M-2002 et M-2003. Commission Géologique du Canada.

Castonguay, S., Dietrich, J., Lavoie, D., and Laliberté, J.-Y., 2010. Structure and petroleum plays of the St. Lawrence Platform and Appalachians in southern Quebec: Insights from interpretation of MRNQ seismic reflection data. Bulletin of Canadian Petroleum Geology, 58 (3), pp. 219-234.

Clark, T.H. and Globensky, Y., 1973. Portneuf et parties de St-Raymond et de Lyster - Comtés de Portneuf et de Lotbinière. Ministère des Richesses Naturelles - Direction Générale des Mines.

Clark, T.H. and Globensky, Y., 1976. Région de Bécancour. Ministère des Richesses Naturelles - Direction Générale des Mines.

Crow, H.L, Ladevèze, P., Laurencelle, M., Benoit, N., Rivard, C., and Lefebvre, R., 2013. Downhole geophysical logging and preliminary analyses of bedrock structural data for groundwater applications in the Montérégie Est area, Québec; Geological Survey of Canada, Open File 7077. doi:10.4095/292295 http://ftp2.cits.rncan.gc.ca/pub/geott/ess_pubs/292/292295/of_7077.zip [accessed June 2015]

Crow, H., Raynauld, M., Lefebvre, R., Gloaguen, E., Brewer, K., and Cartwright, T. 2014. Borehole geophysical studies in a fractured sedimentary rock aquifer in Haldimand, Gaspé, Québec; Geological Survey of Canada, Open File 7492. doi:10.4095/293363 http://ftp2.cits.rncan.gc.ca/pub/geott/ess_pubs/293/293363/of_7492.zip [accessed June 2015]

Comeau, F.A., Kirkwood, D., Malo, M., Asselin, E. and Bertrand, R., 2004. Taconian mélanges in the parautochthonous zone of the Quebec Appalachians revisited: implications for foreland basin and thrust belt evolution. Canadian Journal of Earth Sciences, 41(12): 1473-1490.

Daniels, J. J., Cole, D., Murphy, M., Welch, S., and Sheets, J., 2011, Mineralogical and physical property characteristics of the Utica-Point Pleasant shale from core and geophysical log analysis; *in* Taking a deeper look at shales: Geology and potential of the Upper Ordovician Utica Shale in the Appalachian basin. Petroleum Technology Transfer Council, Ohio Geological Survey, and Ohio Geological Society, June 21, 2011, New Philadelphia, OH. http://www.thepttc.org/workshops/eastern_062111/eastern_062111_Daniels.pdf [accessed June 2015]

Globensky, Y., 1987. Géologie des Basses Terres du Saint-Laurent. Direction Générale de l'Exploration Géologique et minérale du Québec - Gouvernement du Québec.

Laurencelle, M., Lefebvre, R., Rivard, C., Parent, M., Ladevèze, P., Benoit, N., Carrier, M.-A., 2013. Modeling the evolution of the regional fractured-rock aquifer system in southern Quebec following the last deglaciation. Conference Proceedings, AIH Annual Meeting (Canadian National Chapter), September 29–October 3, 2013,Montreal,Quebec, 8 pp. (ESS Cont.# 20140054)

Lavoie, D., 2008. Chapter 3 Appalachian Foreland Basin of Canada. In: D.M. Andrew (Editor), Sedimentary Basins of the World. Elsevier, pp. 65-103.

Lavoie, D., Rivard, C., Lefebvre, R., Séjourné, S., Thériault, R., Duchesne, M.J., Ahad, J.M.E., Wang, B., Benoit, N., Lamontagne, C., 2014. The Utica Shale and gas play in southern Quebec: Geological and hydrogeological syntheses and methodological approaches to groundwater risk evaluation, International Journal of Coal Geology, 126, pp. 77-91.

MDDELCC, 2014. Charactérisation hydrogéologique du secteur Haldimand, rapport final; Institut national de la recherche scientifique - Centre Eau Terre Environnement (INRS-ETE); Rapport de recherche R-1497, 229p. http://www.mddelcc.gouv.qc.ca/eau/Rapport-Haldimand/Haldimand_Rapport.pdf [accessed June 2015]

Molgat, M. 2011. Shale Gas Potential in the Quebec Lowlands; High Potential in a New Frontiers Area; *in* Taking a deeper look at shales: Geology and potential of the Upper Ordovician Utica Shale in the Appalachian basin. Petroleum Technology Transfer Council, Ohio Geological Survey, and Ohio Geological Society, June 21, 2011, New Philadelphia, OH. http://www.thepttc.org/workshops/eastern_062111/eastern_062111_Molgat.pdf [accessed June 2015]

Raynauld, M. Crow, H., Fagnan, N.; Lefebvre, R.; Molson, J. Gloaguen, E.; Benoit, N. 2013. Caractérisation des conditions hydrogéologiques au-dessus du réservoir pétrolier de Haldimand, Gaspé, Québec; In proceedings: Géomontreal 2013 - 66th Annual Canadian Geotechnical, Conference and 11th Joint CGS/IAH-CNC Groundwater Conference, Montreal, Canada, September 29th - October 3, 2013.

Séjourné, S., Dietrich, J. and Malo, M., 2003. Seismic characterization of the structural front of southern Quebec Appalachians. Bulletin of Canadian Petroleum Geology, 51(1): 29-44.

Séjourné, S., 2015 Étude des log acoustiques série F – Région de St-Édouard; internal report submitted 2015 (in prep)

St.-Julien, P. and Hubert, C., 1975. Evolution of the Taconian orogen in the Quebec Appalachians. American Journal of Science, 275-A: 337-362.

St.-Julien, P., Slivitsky, A. and Feininger, T., 1983. A deep structural profile across the Appalachians of southern Quebec. Geological Society of America Memoirs, 158: 103-112.

Thériault, R. and Beauséjour, S., 2012. Carte géologique du Québec, Edition 2012. Ressources Naturelles Québec, DV 2012-07.

Williams, H., 1979. Appalachian Orogen in Canada. Canadian Journal of Earth Sciences, 16(3): 792-807

Appendix A – Geophysical Log Background

Appendix A provides background information on the downhole logging methods used in the Montérégie Est area, and Appendix B presents the interpreted figures of the log suites.

Gamma Methods

Natural gamma logging (or gamma ray logging) detects the presence of naturally occurring or man-made radioactive isotopes. The most common naturally-occurring isotopes in rock and soil are potassium (K), uranium (U), and thorium (Th), the most common being potassium in rock forming minerals.

Natural gamma logging tools measure radioactivity by converting gamma rays (photons) emitted from the formation into electronic pulses using a scintillator crystal (detector) in the tool. For total count gamma logging, it is sufficient to count the total number of pulses per second. Radioactive decay is statistical in nature and photon emission follows a Poisson's distribution. The standard deviation of the count number will be its square root. The accuracy of the measurement is greatest at high count rates over slower logging speeds, therefore, it is preferable to maintain a very low logging speed.

Instrument response (count rate) varies as the tool moves past lithological changes intersected by the borehole. The most common uses for the gamma logs are for the identification of lithological changes and stratigraphic correlation from hole-to-hole. Typically, count rates are more elevated in finer grained rocks (shales) and decrease with increasing grainsize.

Electrical Methods

The **guard resistivity** log, a type of focused-resistivity measurement, is designed to identify the boundaries of thin beds and measure their resistivity, even in the presence of highly conductive fluids (Keys, 1997; Hearst, 2000). As opposed to induction methods, the guard tool comes into direct contact with the borehole walls and is run in open boreholes. A button electrode on the side of the tool emits a small AC current (50 μs) into the formation. The tool body forms the guard electrode which maintains a constant potential surface, forcing the current out into the rocks surrounding the well and diminishing any current flow along the wellbore. The result is a focused resistivity measurement with a vertical resolution of approximately 2.5 cm (Mount Sopris, 2009). This tool provides qualitative resistivity values, not a true resistivity measurement.

Hearst, J.R., Nelson, P.H. and Paillet, F.L., 2000. Well Logging for Physical Properties; John Wiley and Sons Ltd., England, 483 p.

Keys, W.S., 1997. A practical guide to borehole geophysics in environmental investigations; CRC Press Inc., Boca Raton, FL., 176 p.

Mount Sopris Instruments, 2009. 2GDA-1000 DX Series Dual Density/Guard/Caliper Probe Manual, Mount Sopris Instruments Co. Inc., Golden Colorado, rev. August 7, 2009.

Fluid Logging Methods

Fluid Temperature/Conductivity

For this project, the GSC used a Mount Sopris dual **fluid temperature / fluid conductivity** probe (model QL-FTC) where both sensors are mounted in the nose of the tool. Temperature is measured using a linear, fast-response semi-conductor with a resolution of 0.01ºC and a range of -20 to 80 ºC. Conductivity is measured using a seven electrode mirrored Wenner array with a range of 5 µS/cm (fresh) to 50 mS/m (saline). Fluid conductivities are compensated for temperature and recorded as measured, and corrected to 20 ºC and 25 ºC. Downhole measured values were compared with samples of groundwater brought to surface and measured immediately with a calibrated hand-held conductivity meter also corrected to 25ºC. This ensured highly accurate measurements were made at each well site.

To be effective in environments where vertical flow is very slight, the fluid tool must be the first probe to enter the borehole after the borehole has stabilized for at least 24 hours, and the log must be recorded in the down direction. Slow logging speeds prevent mixing of the fluid ahead of the probe and allow time for the thermistor to react to slight changes in temperature. Gradient calculations (dT/dz) assist in identifying zones where fluctuations occur over very small changes in temperature.

Heat Pulse Flowmeter

Many methods have been developed over recent decades to measure vertical fluid flow along an open borehole or well screen for groundwater applications. These methods have included impellers, tracer-release methods, thermal-pulse flowmeters, and electromagnetic (EM) flowmeters. Thermal and EM vertical component flowmeters are quite sensitive in low-flow conditions, permitting high-resolution measurement of the ambient vertical flow in natural or pumped borehole environments. Ambient flow measurements provide information on the direction of the vertical component of the hydraulic gradient and the location of hydraulically active features in fractured bedrock. Measurements made under artificial pumping conditions provide information on the relative differences in the permeability of targeted bedrock zones or fractures.

The **heat pulse flowmeter** used in these surveys (HFM-2293 manufactured by Mount Sopris Instrument Co.) is based on a US Geological Survey design to measure low-velocity flow environments (Hess, 1982, 1986). This flowmeter contains a heating grid with equidistant temperature sensors positioned a few centimetres above and below the grid. Rubber diverter petals centralize and seal the probe in the borehole, forcing the fluid to pass through a wire mesh over the heating grid and the sensors. When the tool is in position for a series of readings, a heat pulse is triggered by the user on a laptop computer. The grid heats a lens of water that moves up or down with the flow of the borehole fluid past either the upper or lower sensor. An amplifier detects the difference in temperature between the sensors, and converts the output to a frequency which is sent up the cable and recorded by the laptop. The software records the time elapsed between when the hest pulse was triggered and when the sensor records the peak temperature change, carried by the flow.

If natural flow is not detectable in the borehole (i.e. <0.110 L/min), artificial upward flow can be induced with a submersible pump to determine the relative flow drawn from permeable fractures. Flow rate must be carefully monitored every few minutes on surface using a graded container and a stopwatch, while water levels are measured in the borehole using a water level meter. This ensures the change in flow rate measured by the tool can be attributed to changes in hydraulic conductivity of the rock mass and not to changes in the pumping rate. The pump's flow rate must be carefully adjusted so

it does not exceed the tool's upper limit of 3.78 L/min, and also to equalize the pumping rate with the recharge (i.e. no measurable drop in water level during the pumping). In non-hydraulically conductive boreholes, reaching stability is very difficult, and sometimes not possible. In these cases, the flow results are converted from a volumetric value, to a percentage of the total pumping rate measured simultaneously at the surface during the downhole flow measurement.

Flowmeter measurements are influenced by number of factors, including the construction and degree of development of a well, and the natural hydrogeological conditions: factors which can change over time. Logging conditions during the test will also influence the results. Proper sealing with the tool's rubber diverters is critical, as a poor seal caused by borehole wall enlargements (such as in fractures or washouts) will influence flow determinations. Collecting caliper and fluid temperature/fluid conductivity logs before flowmeter logging guides the selection of test intervals. Allowing sufficient time for the fluid to settle after moving the tool in the borehole is also critical, particularly in wells with very low ambient flows.

Hess, A. E., 1982. A heat-pulse flowmeter for measuring low velocities in boreholes, U.S. Geological Survey Open-File Report 82-699, U.S. Geological Survey, Reston, Virginia.

Hess, A. E., 1986. Identifying hydraulically conductive fractures with a slow-velocity borehole flowmeter, Canadian Geotechnical Journal, 23:69-78.

Imaging Methods

Televiewers provide a method of imaging the inside of the borehole wall in very high resolution, either using ultrasonic pulses (acoustic televiewer, ATV), or digital color scans (optical televiewer, OTV).

Both televiewers are equipped with an APS544 orientation sensor, containing a 3-axis magnetometer and 3 accelerometers, to constantly resolve magnetic north and the tilt of the tool. Each line scan contains the direction of magnetic north, and also the tilt of the borehole at that depth. The tool can resolve azimuth with an accuracy of 1°, and tilt to an accuracy of 0.5°. When the televiewer images are imported into processing software, they can be oriented to magnetic north (or to the high side of the borehole in the case of inclined borings). Once the dip and dip direction of structural features are interpreted, they can be corrected for any tilt of the borehole from vertical.

Centralization is key in the collection of high quality images, particularly with the ATV. The tool is kept centered in the borehole with the use of two or more bowspring arm centralizers, made of non-magnetic material, fixed to the tool's housing.

Acoustic Televiewer (ATV)

The ATV transmits a pulse from a fixed transducer and a rotating focusing mirror, and records the amplitude and traveltime of the signal reflected by the borehole wall. The ATV used in these surveys (the ABI40, manufactured by Advanced Logic Technology SA.) records the entire reflected wavetrain, and processing algorithms allow the software in real time to determine the first reflection from the tool's acoustic window, the bedrock wall, and all other subsequent reflections.

Line scans of the borehole wall are collected in intervals as small as 1mm, and at a resolution as high as 288 pixels/revolution. The number of pixels per degree will depend on the diameter of the borehole. To collect images this detailed, the tool must be run very slowly (~1m/min) however a slight decrease

in quality (i.e. 2mm intervals and/or fewer pixels/rev) can allow for a faster logging speed (~2-3m/min).

The ATV's traveltime image can be processed to build a 360° caliper of the borehole shape. This can then serve as a mesh around which the amplitude image can be draped to create a 3D image of the borehole. Features such as open fractures and washouts can be better visualized using this technique.

Optical Televiewer (OTV)

The OTV is designed for optical imaging of the surface of open or cased wells in air or clear water. The tool used in these surveys (the OBI40, manufactured by Advanced Logic Technology SA.) is equipped with a high sensitivity charge-coupled device (CCD) digital camera with Pentax optics. The stationary camera is located above a conical mirror which spins during logging and captures the reflection of the borehole wall. Light for the recording is provided by an LED ring of user configurable intensity depending on the color of the bedrock.

Line scans of the borehole wall are collected in intervals as small as 1 mm, and at a resolution as high as 1.25 pixels/degree. The number of pixels per degree will depend on the diameter of the borehole. To collect images this detailed, the tool must be run slowly (~1.5 m/min) however a slight decrease in quality (i.e. 2 mm intervals and/or fewer pixels/rev) can allow for a faster logging speed (~2-3 m/min).

Appendix B – Geophysical log suites

Borehole:	F-1	Easting:	281 384 m	Depth Drilled:	49.7 m	Logged:	Oct 20-21, 2013
Location:	Ste-Croix, QC	Northing:	5 168 971 m	Method:	Diamond drill	Water Level:	0.27 m
Project:	Shale Gas	UTM Zone:	19	Diameter:	96 mm	Casing:	Steel in overburden
Program:	Environmental Geoscience	Datum:	WGS84	Stick up:	0.90 m		

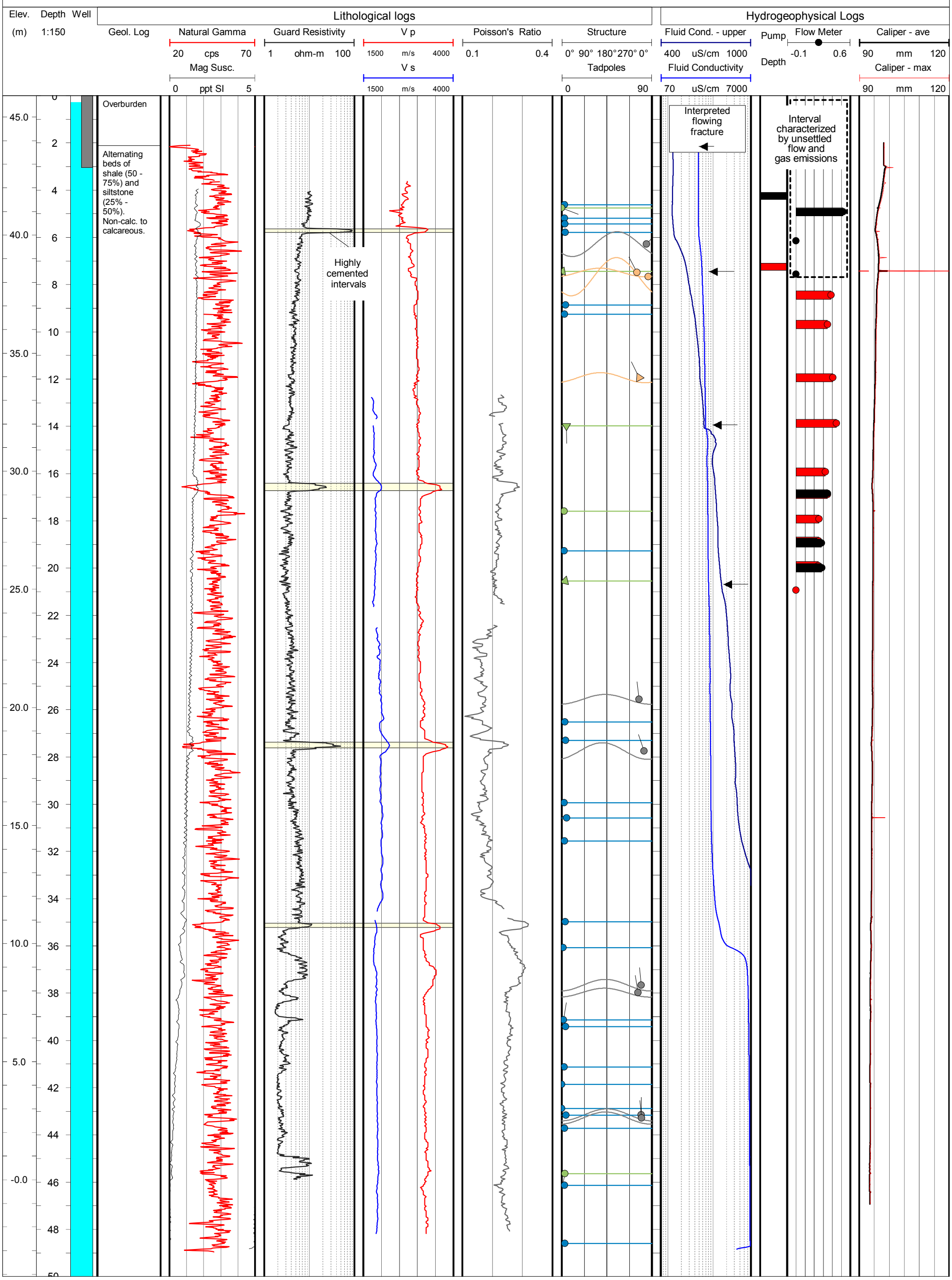

Borehole:	F-2	Easting:	287 925 m	Depth Drilled:	52.1 m	Logged:	Nov 4, 10, 2014
Location:	St-Édouard, QC	Northing:	5 155 391 m	Method:	Diamond drill	Water Level:	2.39 m bgl
Project:	Shale Gas	UTM Zone:	19	Diameter:	96 mm	Casing:	Steel in overburden
Program:	Environmental Geoscience	Datum:	WGS84	Stick up:	0.98 m		

Elev. (m) | Depth 1:150 | Well | Lithological logs | Hydrogeophysical Logs

Geol. Log | Natural Gamma 20 cps 70 | Guard Res. 1 ohm-m 1000 | V p 1000 4000 | V s 1000 4000 | Poisson's Ratio 0.1 0.4 | Structure 0° 90° 180° 270° 0° Tadpoles 0 90 | Fluid Cond. (25'C) 350 uS/cm 650 Fluid Temp. 6.5 deg C 7.1 | Pump Depth | Fluid Flow 0 L/min 1 | Caliper - Average 90 mm 180 Caliper - Max 90 mm 180

Overburden

Dark grey shale containing black laminations. Brechified and fractued in many intervals, Lightly calcarous to calcareous. Calcite veins present in some fracture zones.

Note:

Log collected in 2013 where obstruction encountered at 29.8 m. Hole reopened in 2014 and surface casing was advanced from 6.35 to 8.13 m. Gamma was not recollected due to time contraints.

Interpreted flowing fracture

Interpreted fractured/ shear zone

Obstruction at 18.3 m

Borehole:	F-3	Easting:	282 584 m	Depth Drilled:	49.9 m	Logged:	Oct 24-25, 2013
Location:	St.-Edouard, QC	Northing:	5 158 820 m	Method:	Diamond drill	Water Level:	1.18 m bgl
Project:	Shale Gas	UTM Zone:	19	Diameter:	96 mm	Casing:	Steel in overburden
Program:	Environmental Geoscience	Datum:	WGS84	Stick up:	0.80 m		

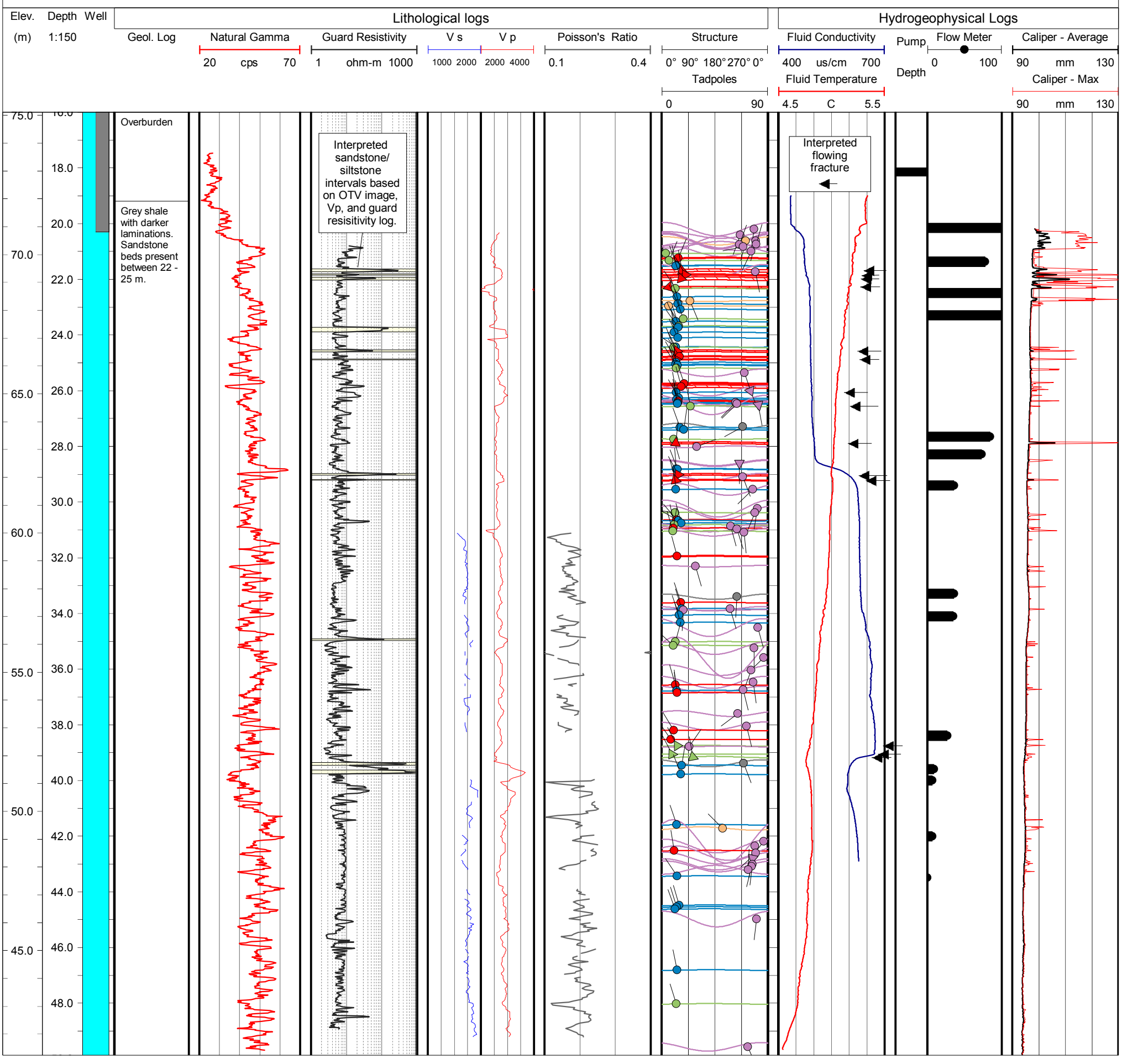

Borehole:	F-4	Easting:	288 214 m	Depth Drilled:	60.4 m	Logged:	Oct '13 / Nov '14
Location:	St.-Edouard, QC	Northing:	5 157 504 m	Method:	Diamond drill	Water Level:	7.52 m (2014)
Project:	Shale Gas	UTM Zone:	19	Diameter:	96 mm	Casing:	Steel in overburden
Program:	Environmental Geoscience	Datum:	WGS84	Stick up:	1.02 m		

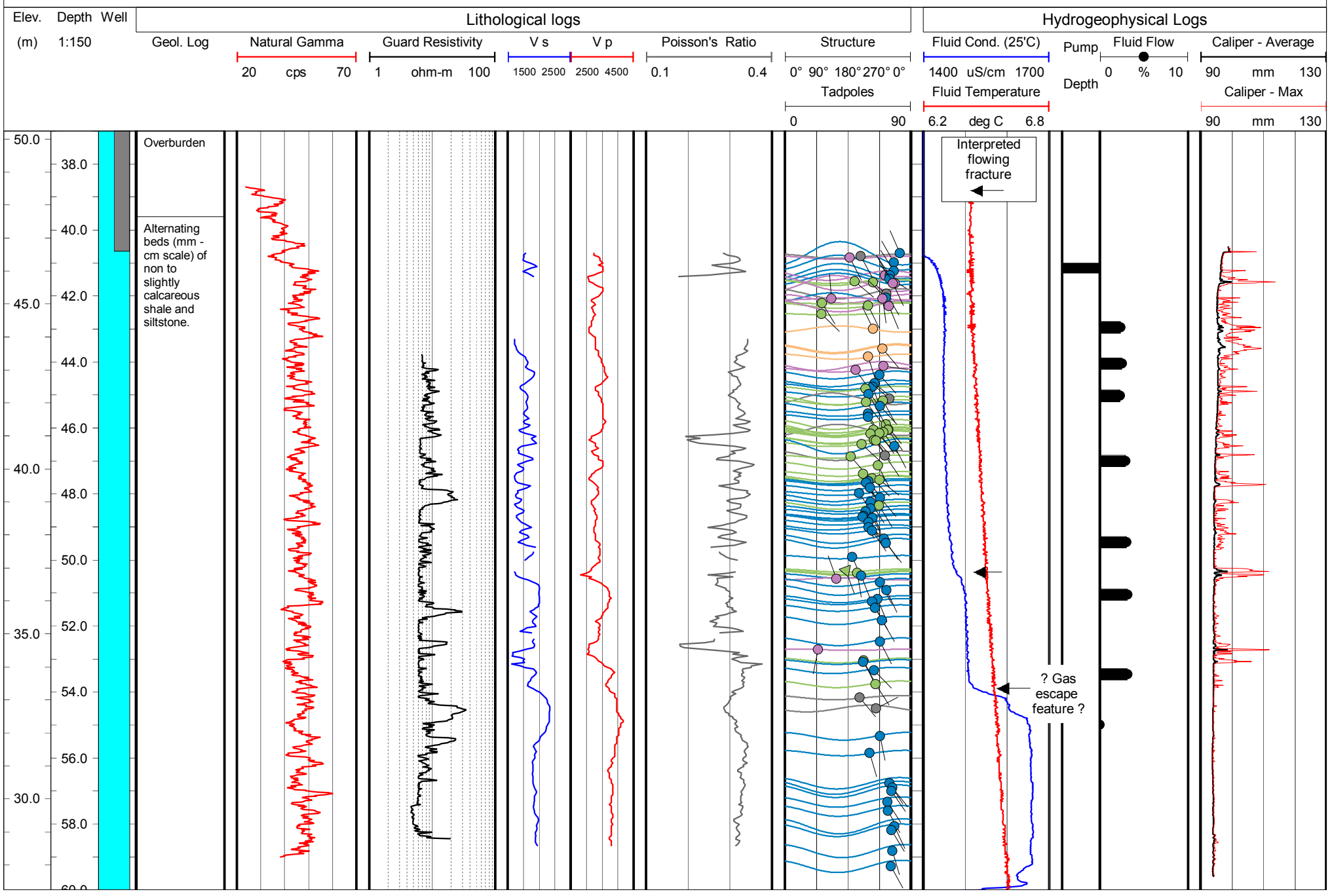

Borehole:	F-7	Easting:	276 263 m	Depth Drilled:	51.5 m	Logged:	Nov 8-9, 2014
Location:	St-Édouard, QC	Northing:	5 164 099 m	Method:	Diamond drill	Water Level:	3.59 m bgl
Project:	Shale Gas	UTM Zone:	19	Diameter:	96 mm	Casing:	Steel in overburden
Program:	Environmental Geoscience	Datum:	WGS84	Stick up:	0.81 m		

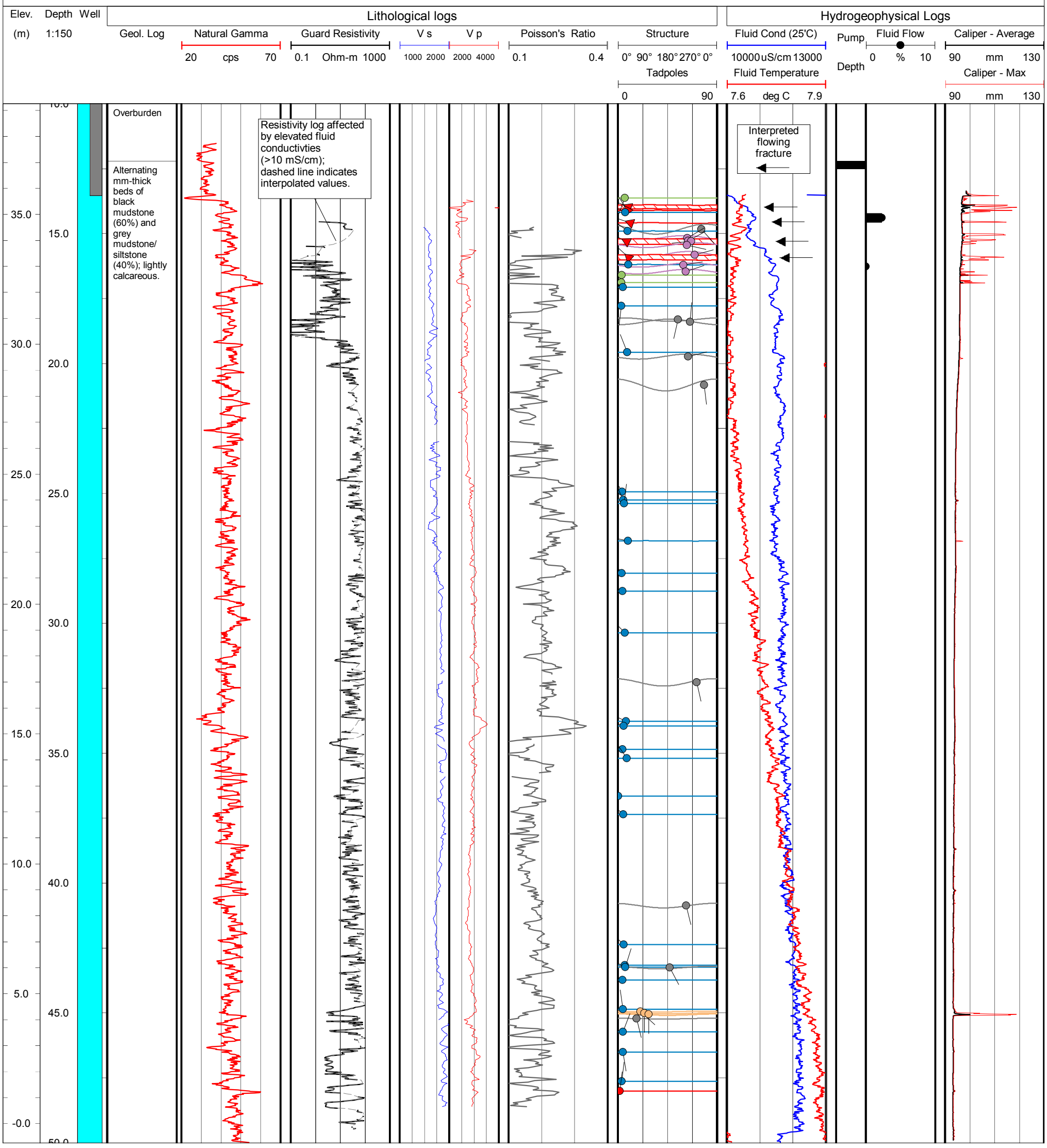

Borehole:	F-8	Easting:	277 620 m	Depth Drilled:	51.5 m	Logged:	Nov 4, 5, 2014
Location:	St-Édouard, QC	Northing:	5 162 758 m	Method:	Diamond drill	Water Level:	0.70 m bgl
Project:	Shale Gas	UTM Zone:	19	Diameter:	96 mm	Casing:	Steel in overburden
Program:	Environmental Geoscience	Datum:	WGS84	Stick up:	0.70 m		

Elev. (m) | Depth 1:150 | Well

Lithological logs

Geol. Log

Natural Gamma: 20 cps 70

Guard Resistivity: 1 ohm-m 100

V s: 1500 2500

V p: 2500 4500

Poisson's Ratio: 0.1 0.4

Structure: 0° 90° 180° 270° 0°

Tadpoles: 0 90

Hydrogeophysical Logs

Caliper - Max: 90 mm 150

Caliper - Average: 90 mm 150

Pump Depth

Flow Meter: 0 10

Fluid Temperature: 7.5 deg C 11.5

Fluid Cond (25'C): 350 uS/cm 450

Overburden

Alternating black mudstone with mm-scale laminations of grey calcareous siltstone. Occ. cm-thick grey sandstone beds.

Interpreted flowing fracture

Borehole:	F-10	Easting:	286 446 m	Depth Drilled:	30.5 m	Logged:	Nov 7, 2014
Location:	St.-Édouard, QC	Northing:	5 157 069 m	Method:	Hammer	Water Level:	1.11 m bgl
Project:	Shale Gas	UTM Zone:	19	Diameter:	152 mm	Casing:	Steel in overburden
Program:	Environmental Geoscience	Datum:	WGS84	Stick up:	0.88 m		

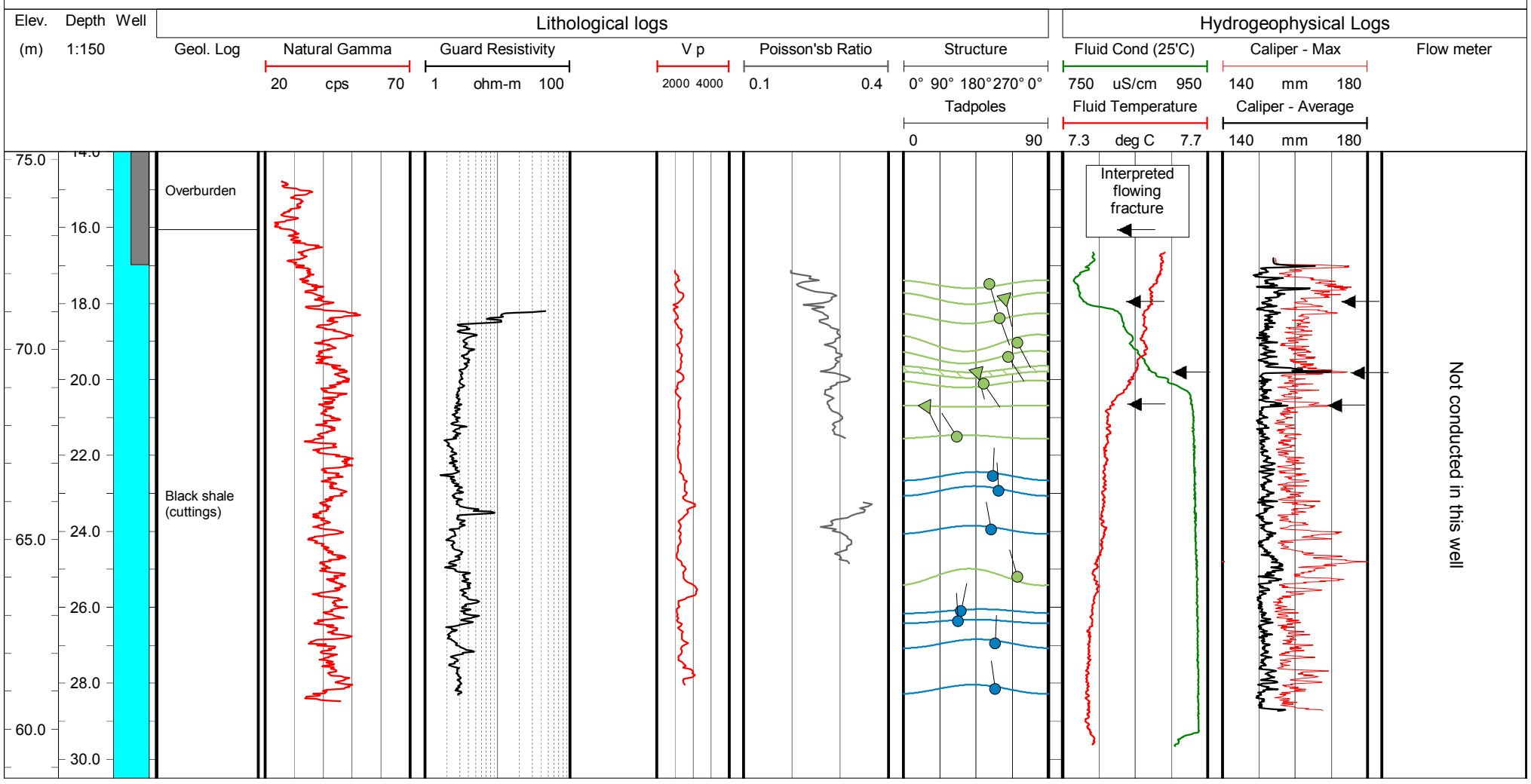

Borehole:	F-11	Easting:	286 409 m	Depth Drilled:	54.9 m	Logged:	Nov 11, 2014
Location:	St-Édouard, QC	Northing:	5 156 769 m	Method:	Hammer	Water Level:	1.88 m bgl
Project:	Shale Gas	UTM Zone:	19	Diameter:	152 mm	Casing:	Steel in overburden
Program:	Environmental Geoscience	Datum:	WGS84	Stick up:	0.85 m		

Elev. (m) | Depth 1:150 | Well

Lithological logs

Geol. Log

Natural Gamma: 20 cps 70

Guard Resistivity: 1 ohm-m 100

V s / V p: 1500 2500 / 2000 4000

Poisson's Ratio: 0.1 0.4

Structure: 0° 90° 180° 270° 0°

Tadpoles: 0 90

Hydrogeophysical Logs

Fluid Cond (25'C): 400 uS/cm 900

Fluid Temperature: 6.5 deg C 8.5

Pump / Flow meter: 0 % 30

Depth

Caliper - Average: 140 mm 200

Caliper - Max: 140 mm 200

Overburden

Black shale with fractures (cuttings)

Interpreted flowing fracture

Flow meter poorly sealed in this interval due to enlarged BH diameter

Caliper exceeds 260 mm

Tools encounter obstruction at 46 m.

Borehole:	F-12	Easting:	286 596 m	Depth Drilled:	73.15 m	Logged:	Nov 10, 2014
Location:	St-Édouard, QC	Northing:	5 156 888 m	Method:	Hammer	Water Level:	0.87 m bgl
Project:	Shale Gas	UTM Zone:	19	Diameter:	152 mm	Casing:	Steel in overburden
Program:	Environmental Geoscience	Datum:	WGS84	Stick up:	0.99 m		

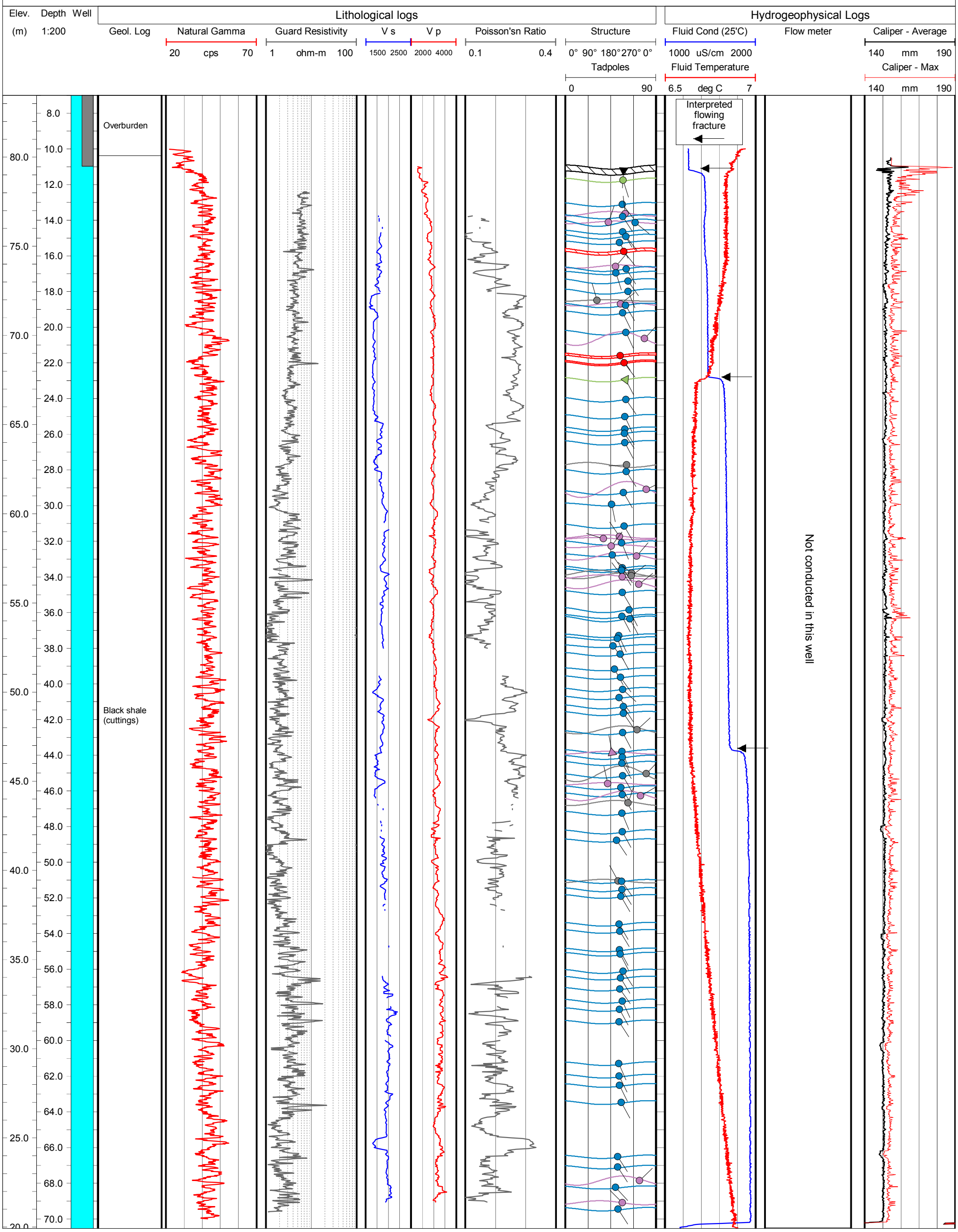

Borehole:	F-13	Easting:	286 797 m	Depth Drilled:	60.96	Logged:	Nov 6, 2014
Location:	St-Édouard, QC	Northing:	5 156 646 m	Method:	Hammer	Water Level:	0.84 m bgl
Project:	Shale Gas	UTM Zone:	19	Diameter:	152 mm	Casing:	Steel in overburden
Program:	Environmental Geoscience	Datum:	WGS84	Stick up:	0.96 m		

Elev. (m) | Depth 1:150 | Well

Lithological logs

Geophys. | Natural Gamma 20 cps 80 | Guard Resistivity 1 ohm-m 100 | V s | V p | Poisson's Ratio 0.1 0.4 | Structure 0° 90° 180° 270° 0°

Interp. | Tadpoles 0 90

Hydrogeophysical Logs

Fluid Temperature 6.5 deg C 10 | Caliper - Average 140 mm 240 | Flow meter

Fluid Cond (25'C) 800 uS/cm 900 | Caliper - Max 140 mm 240

Overburden

Black shale (cuttings)

Zone of interpreted finer grained, softer rock (increased gamma cps coupled with lower velocity and increased caliper)

Interpreted flowing fracture

Caliper exceeds 260 mm

Not conducted in this well

Borehole:	F-21	Easting:	287 008 m	Depth Drilled:	152.1 m	Logged:	Nov 1-3, 2014
Location:	St.-Édouard, QC	Northing:	5 156 395 m	Method:	Diamond drill	Water Level:	1.53 m bgl
Project:	Shale Gas	UTM Zone:	19	Diameter:	96 mm	Casing:	Steel in overburden
Program:	Environmental Geoscience	Datum:	WGS84	Stick up:	0.84 m		

Elev. (m) | Depth 1:400 | Well

Lithological logs

Geol. Log

Natural Gamma: 20 cps 70

Guard Resistivity: 1 ohm-m 100

V s / V p: 1000 2500 / 2000 5000

Poisson's Ratio: 0.1 0.4

Structure: 0° 90° 180° 270° 0°

Tadpoles: 0 90

Hydrogeophysical Logs

Fluid Temperature: 6.6 deg C 8.2

Fluid Conductivity: 400 uS/cm 4000

Pump Depth

Fluid Flow: -50 % 50

Caliper - Max: 80 mm 160

Caliper - Average: 80 mm 160

Black calcareous shale with 10-15% mm-scale light grey laminations, interbedded with black calcareous mudstone with mm-scale silty laminations. Core indicates rock is deformed. 10% of interval is brecciated and contains calcite veins and veinlets with silicious cement.

Black shale containing 10-15% mm-scale light grey laminations. Core indicates deformation and contains a calcite-filled fracture. Cm-scale brecciated intervals make up 10% of interval. Veinlets contain silicious cement.

Folded black shale with fine, mm-scale laminations of variable thickness (5 - 25% of interval). Lightly calcareous and glossy. Locally abundant fissures filled with calcite.

Highly cemented intervals

Interpreted flowing fracture

Zone of anomalous vertical flow during pump test; numerous potentially flowing fractures

Interpreted fractured/ shear zone